REDUCED-ORDER MODELING AND CONTROL OF PEM FUEL CELLS VIA BALANCING TRANSFORMATION AND SINGULAR PERTURBATIONS

By

KLITI KODRA

A thesis submitted to the

Graduate School-New Brunswick

Rutgers, The State University of New Jersey

in partial fulfillment of the requirements

for the degree of

Master of Science

Graduate Program in Electrical and Computer Engineering

written under the direction of

Dr. Zoran Gajic

and approved by

_____

_____

_____

_____

New Brunswick, New Jersey

OCTOBER 2012

ABSTRACT OF THE THESIS

Reduced-order Modeling and Control of PEM Fuel Cells via Balancing Transformation and Singular Perturbations

by KLITI KODRA

Thesis Director: Dr. Zoran Gajic

Fuel cell systems are considered important clean energy sources with great potential for the future. The mathematical models of fuel cell – fuel processing systems (FC – FPS) are quite complex therefore it is important to simplify them for efficient study. In this thesis we apply order-reduction techniques to replace a large scale model with a much smaller one while still retaining the original behavior.

Two order-reduction techniques, namely, the balancing transformation and balancing residualization applied to an 18^{th}-order FC – FPS model are investigated in the first part of the study. The results show that the reduced system even down to 5^{th}-order still retains the original dynamics.

In the second part of the thesis we demonstrate how to put linear system in singularly perturbed form and then investigate the approximate gramians and balancing transformation of the reduced-order system. For the linear singularly perturbed system in explicit form we provide a method to evaluate the exact gramians in terms of pure slow and pure fast reduced-order Lyapunov algebraic equations and improve the approximate method available in the control literature for order-reduction of singularly perturbed systems via balancing transformation.

Acknowledgements

I am very grateful to a lot of people for supporting me to complete this work. Special thanks go to my adviser Dr. Zoran Gajic for his continuous help and suggestions during the research process. I would also like to thank my thesis committee members Dr. Dario Pompili, Dr. Predrag Spasojevic, and Dr. Ehad Shoubaki for their valuable comments.

I cannot forget to express my gratitude to the Electrical and Computer Engineering Department at Rutgers University for the financial support that they have been providing me for the past two years.

Last but not least I would also like to thank my parents without whom this would have not been possible.

Table of Contents

List of Tables

List of Illustrations

Chapter 1

1. Introduction

Most of the global energy at the present is generated by using fossil fuels and nuclear power. While the demand is met, these sources are neither sustainable nor renewable and they have potential consequences for humans and the environment alike. An important enabling technology that might have the potential to revolutionize the way we power our planet in a cleaner and more efficient way is the fuel cell. Fuel cells have the capability of replacing the internal-combustion engine in vehicles and provide power in stationary and portable applications. Another advantage of the fuel cells is that they do not emit any greenhouse gases or pollutants at the point of operation i.e. if pure hydrogen is used as a fuel, fuel cells emit only heat and water as byproducts. Currently most of the hydrogen fuel is obtained via natural gas reforming which is quite efficient (up to 55%) and it primarily uses fossil fuels during the reforming process. The reformer will have to be addressed accordingly if fuel cells are going to be major players in power generation in the years to come. Additionally, another challenge is the high capital cost associated with fuel cells. That has been the main obstacle responsible for the limited market penetration of fuel cell technology. Nonetheless, there is promising research showing that technical and non-technical barriers will be overcome in the near future hence leading to the widespread use of fuel cells technologies.

1.1 The Fuel Cell

In a nutshell, the fuel cell is an electrochemical device that converts chemical energy into electrical energy without generating greenhouse gases or other pollutants. It is a

simple triode made of the anode, the membrane and the cathode. While there are different types of fuel cells the most commonly used are the Proton Exchange Membrane Fuel Cell (PEMFC) and the Solid Oxide Fuel Cell (SOFC). The PEMFC is the most developed fuel cell so far and it is mainly used in transportation, backup power, and residential power generation. SOFC applications fall primarily into distributed electric power generation. In this thesis we will focus only on the PEMFC. Table 1 compares four main characteristics of PEMFC and SOFC.

Table 1: PEMFC vs. SOFC

	PEM	SOFC
Efficiency (%)	40 – 50	50 – 60
Operating Temperature (˚C)	50 – 100 (Typically 80)	600 - 1000
Dynamics	Faster	Slower
Power Range	1 kW – 1MW	5 kW – 5 MW

1.1.1 PEMFC Principle of Operation

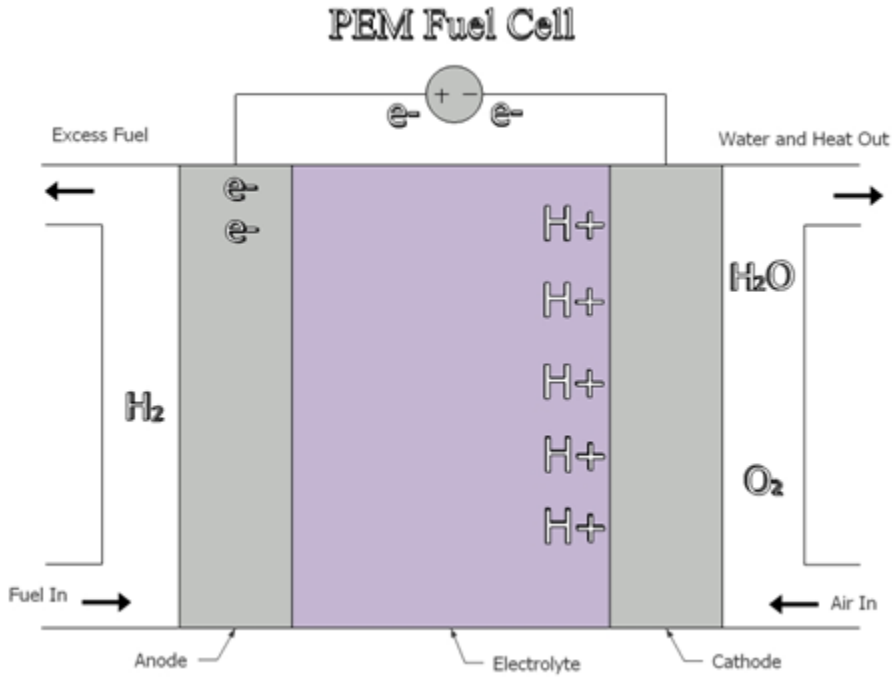

Figure 1. PEMFC diagram

The PEMFC was invented in the 1960s but the principle of its operation was discovered circa 1840 [19]. The process starts with the hydrogen delivery to the anode side where it is catalytically split into electrons and protons. During this process the membrane, which is a solid, teflon-like material, plays a critical role in the chemical reaction because it serves as a conductor for protons and as an isolator for electrons. The electrons travel through an external circuit to the cathode thus creating an output current. The protons on the other hand permeate through the polymer electrolyte membrane to the cathode side where they combine with a stream of oxygen releasing water in the process. The chemical equations at the anode and cathode respectively are

$$2H_2 \rightarrow 4H^+ + 4e^- \tag{1.1}$$

$$4H^+ + 4e^- + O_2 \rightarrow 2H_2 \tag{1.2}$$

To ensure optimal performance, prevent the damage of the membrane, and maintain a high efficiency it is important to practice the following:

- Air must be cooled down to the operating temperature (< 80˚C)
- An optimal supply of hydrogen must be provided on the anode side
- An optimal supply of oxygen must be provided on the cathode side
- Effective water and heat management

1.2 The Reformer

In this section we give a brief introduction to the steam methane reformer since the thesis is focused on the fuel cell – reformer system rather than just the fuel cell.

A reformer is a device that produces hydrogen from fossil fuels such as methane. The most common one used widely in industry is the steam methane reformer. The process

happens at high temperatures and in the presence of a metal-based catalyst. Methane reacts with steam to yield carbon monoxide and water as described by (1.3).

$$CH_4 + H_2O \rightarrow 3H_2 + CO \tag{1.3}$$

The reaction of (1.3) is strongly endothermic. More hydrogen can be obtained by combining the carbon monoxide with water in what is called a water gas-shift reaction (WGS). This exothermic process is summarized by (1.4).

$$CO + H_2O \rightarrow CO_2 + H_2 \tag{1.4}$$

In essence, during reforming natural gas is mixed with air and passed to the main reactor called the catalytic partial oxidation (CPOX) reactor. The gas coming out of the CPOX reactor containing primarily H_2, CO, CO_2, H_2O, and N_2 is cooled down using water and is sent through two WGS reactors to remove excess CO_2. Water injection during this stage serves not only to bring the temperature down to the required inlet temperature for the WGS reactors but also to increase the moisture content (steam-to-carbon ratio) and drive the WGS reaction forward [33]. The reformate from the WGS reactors is further cooled down and mixed with air to clean up additional CO in the preferential oxidation reaction (PROX) [33]. At this point the hydrogen is ready to be fed to the PEM. Figure 2 shows the step-by-step process described above.

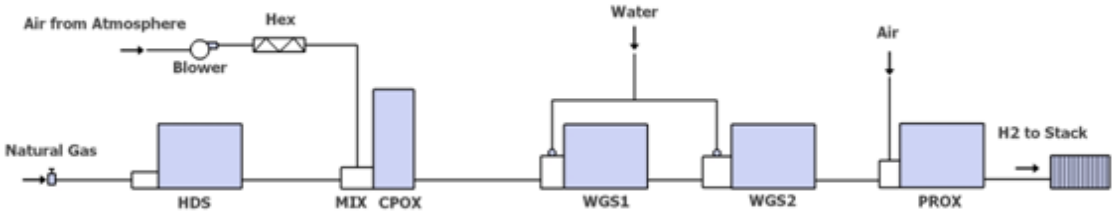

Figure 2. Reformer components

1.3 Thesis Overview

Chapter 1 is an introductory chapter containing the fundamentals of some of the tools such as balancing realization and the theory of singular perturbations that will be used throughout the thesis. In Chapter 2 we investigate the linearized fuel cell and the fuel cell – reformer models (given in Pukrushpan et al [15], [31] – [34]) separately. We perform system order reduction to the fuel cell – reformer linearized models using two techniques: direct truncation of the balanced system and the balancing residualization technique. Here we compare the impulse and step responses and also investigate frequency behavior obtained using both techniques. Additionally, we also conclude that the optimal performance remains unchanged under balanced coordinates. Likewise, we show that the continuous algebraic Ricatti equation (CARE) is preserved during a similarity transformation. In Chapter 3 we apply the technique devised by Shahruz and Behtash [3] to determine an approximate balancing transformation for the full system by computing the balancing transformation for the slow and fast subsystems separately. We take it one step further and decouple the reduced-order Lyapunov differential equation using the famed Chang transformation to obtain an exact value of the balancing transformation using the slow and fast subsystems.

1.4 Modeling the Fuel Cell

Several PEMFC mathematical models have been developed so far. The simplest of them is the 3^{rd} - order linear model derived by El-Sharkh et al. [18]. In this model the dynamics of the PEMFC are described by three variables: pressure of hydrogen, pressure of oxygen, and pressure of the water vapor. The model is given in (1.5).

$$\dot{x}_1(t) = -\frac{1}{\tau_{H_2}} x_1(t) + \frac{1}{\tau_{H_2} K_{H_2}} q_{H_2}^{in}(t) - \frac{2k_r}{\tau_{H_2} K_{H_2}} I(t)$$
$$\dot{x}_2(t) = -\frac{1}{\tau_{O_2}} x_2(t) + \frac{1}{\tau_{O_2} K_{O_2}} q_{O_2}^{in}(t) - \frac{k_r}{\tau_{O_2} K_{O_2}} I(t) \quad (1.5)$$
$$\dot{x}_3(t) = -\frac{1}{\tau_{H_2O}} x_3(t) + \frac{2k_r}{\tau_{H_2O} K_{H_2O}} I(t)$$

The state variables $x_1(t), x_2(t)$ and $x_3(t)$ represent the pressures $p_{H_2}(t)$, $p_{O_2}(t)$ and $p_{H_2O}(t)$ respectively and control variables $q_{H_2}(t)$ and $q_{O_2}(t)$ represent the molar flow rates of hydrogen and oxygen and k_r is a modeling constant $(kmol \cdot (s \cdot A)^{-1})$. The nonlinear output equation which is the measured fuel cell voltage is obtained using the Nernst formula [19]. For the PEMFC, the output voltage is given by

$$y(t) = V(t) = N\left(E_0 + \frac{RT}{2F} ln\left\{\frac{x_1(t)[\, x_2(t)]^{0.5}}{x_3(t)}\right\}\right) - \beta \ln\big(\gamma I(t)\big) - R^{int} I(t) \quad (1.6)$$

The quantities in (1.6) are defined in Table 2.

Table 2: Definition of quantities in Equation (1.6)

Quantity	Definition
N	Number of fuel cells in the stack
E_0	Open cell voltage (V)
R	Universal gas constant $((l \cdot atm) \cdot (kmol \cdot K)^{-1})$
T	Absolute temperature (K)
F	Faraday's constant $(C \cdot kmol^{-1})$
β	Constant (V)
γ	Constant (A^{-1})
R^{int}	Internal resistance (Ω)

The disadvantage of this model is that it is not controllable. The third equation in (1.5) is only affected by the current $I(t)$ which is the system's disturbance and not a controlled variable.

Another fuel cell model is the nonlinear 3rd- order model developed by Chiu et al. [38]. The state variables are the same as in the previous case while the control inputs (u) $W_{H_2}^{in}, W_{O_2}^{in}$ and $W_{H_2Oc}^{in}$ represent the inlet flow rates of the hydrogen on the anode side, oxygen and water in the cathode side. The nonlinear system is given in (1.7).

$$\begin{aligned}\dot{x}_1(t) &= \frac{RT}{V_A}\left(u_1 - \left[u_1 + W_{H_2O_A}^{in} - 2k_rI\right]\frac{x_1}{x_1 + p_{H_2O}} - 2k_rI\right) \\ \dot{x}_2(t) &= \frac{RT}{V_C}\left(u_2 - \left[u_2 + u_3 + W_{N_2}^{in} - k_rI\right]\frac{x_2}{x_2 + x_3 + p_{N_2}} - k_rI\right) \\ \dot{x}_3(t) &= \frac{RT}{V_C}\left(u_3 - \left[u_2 + u_3 + W_{N_2}^{in} - k_rI\right]\frac{x_3}{x_2 + x_3 + p_{N_2}} - 2k_rI\right)\end{aligned} \tag{1.7}$$

The drawback of this model is that it assumes that the constant values of inlet flow rates $W_{H_2O_A}^{in}$, $W_{N_2}^{in}$ and pressures $p_{H_2O_A}$, p_{N_2} are supposed to be known.

Na and Gou [37] developed an improved Chiu model that also studies the dynamics of $H_2O_A^{in}$ and N_2^{in} . The 5th - order nonlinear model is shown in (1.8).

$$\begin{aligned}\dot{x}_1(t) &= \frac{RT}{V_A}\left(Y_{H_2} - \frac{x_1}{x_1 + x_2}\right)k_a u_a + RTC_1\left(\frac{x_1}{x_1 + x_2} - 1\right)I \\ \dot{x}_2(t) &= \frac{RT}{V_A}\left(\frac{x_2}{x_1 + x_2 - \varphi_a P_{vs}} - \frac{k_a x_1}{x_1 + x_2}\right)u_a + \frac{RTC_1}{V_A}\left(\frac{x_1}{x_1 + x_2} - 1\right)I \\ \dot{x}_3(t) &= \frac{RT}{V_C}\left(Y_{O_2} - \frac{x_3}{x_3 + x_4 + x_5}\right)k_c u_c + \frac{RTC_1}{2V_C}\left(\frac{x_2}{x_3 + x_4 + x_5} - 1\right)I \\ \dot{x}_4(t) &= \frac{RT}{V_C}\left(Y_{N_2} - \frac{x_4}{x_3 + x_4 + x_5}\right)k_c u_c \\ \dot{x}_5(t) &= \frac{RT}{V_C}\left(\frac{\varphi_c P_{vs}}{x_3 + x_4 + x_5 + \varphi_c P_{vs}} - \frac{x_4}{x_3 + x_4 + x_5}\right)k_c u_c \\ &\quad + \frac{RT}{V_C}\left(\frac{C_1 x_5}{x_3 + x_4 + x_5} - C_1 - \frac{C_2 x_5}{x_3 + x_4 + x_5} + C_2\right)I\end{aligned} \tag{1.8}$$

Table 3: Definition of quantities in Equation (1.8)

Quantity	Definition
φ_a	Relative humidity at the anode
φ_c	Relative humidity at the cathode
Y	Mole fraction
P_{vs}	Saturation pressure (atm)
k	Modeling constant

The state variables in this model represent respectively the pressures of hydrogen and water at the anode and the pressures of oxygen, nitrogen, and water at the cathode, that is

$$x(t) = \begin{bmatrix} p_{H_2}(t) & p_{H_2O_A}(t) & p_{O_2}(t) & p_{N_2}(t) & p_{H_2O_C}(t) \end{bmatrix}^T \tag{1.9}$$

The output variables are defined by $y(t) = [p_{H_2}(t) \quad p_{O_2}(t)]^T$ and the control input is given by $u(t) = [u_a(t) \quad u_c(t)]^T$ where

$$u_a(t) = \frac{1}{k_a}(H_{2in}(t) + H_2O_{Ain}(t)) \tag{1.10}$$

and

$$u_c(t) = \frac{1}{k_c}(O_{2in}(t) + N_{2in}(t) + H_2O_{Cin}(t)) \tag{1.11}$$

Higher-order nonlinear models of PEMFC have been obtained by Pukrushpan et al [33]. The 9th-order model developed by Pukrushpan will be used for analysis in Chapter 2.

1.5 Fundamentals of Balancing Transformation

Balancing of linear time-invariant systems is a well-known technique used for system order reduction [35]. When a linear system is in balanced form, its Hankel singular values serve as a measure for the dynamic importance of state components. If a Hankel singular value is relatively small, the influence of the corresponding state component on the output and input energy is respectively, low and therefore this state component can be

disregarded in order to obtain a reduced-order system [4], [11]. Let us consider a linear time-invariant system represented by

$$\begin{aligned} \dot{x}(t) &= Ax(t) + Bu(t) \\ y(t) &= Cx(t) + Du(t) \end{aligned} \tag{1.12}$$

In (1.5) $x \in R^n$ is the system state vector, $u \in R^m$ is the system input vector and $y \in R^p$ is the system output vector. The open-loop transfer function is given by

$$G(s) = C(sI - A)^{-1}B + D \tag{1.13}$$

It is assumed that the system is asymptotically stable and that the pairs (A, B) and (A, C) are controllable and observable respectively. Then, using the balancing transformation technique we can put the system into balanced coordinates in which the controllability and observability gramians defined by [8]

$$\begin{aligned} P &:= \int_0^\infty e^{At} B B^T e^{A^T t} dt \\ Q &:= \int_0^\infty e^{A^T t} C^T C e^{At} dt \end{aligned} \tag{1.14}$$

are identical and diagonal. Hence, using the balancing transformation $x_b(t) = Tx(t)$ where $\det(T) \neq 0$, the system in (1.5) becomes

$$\begin{aligned} \dot{x}_b(t) &= A_b x_b(t) + B_b u(t) \\ y_b(t) &= C_b x_b(t) + D_b u(t) \end{aligned} \tag{1.15}$$

The matrices in (1.8) are given by [26]

$$A_b = TAT^{-1}, B_b = TB, C_b = CT^{-1}, D_b = D \tag{1.16}$$

As mentioned above, the following will be true when the system is in the balanced coordinates (σ_i are the Hankel singular values $\sigma_i^2 = \lambda_i(PQ)$)

$$\begin{aligned} P_b = Q_b = \Sigma = diag(\sigma_1, \sigma_2 \ldots \sigma_n) \\ \sigma_1 \geq \sigma_2 \geq \cdots \geq \sigma_n > 0 \end{aligned} \tag{1.17}$$

Furthermore, the gramians P_b and Q_b are the unique solutions of the following algebraic Lyapunov equations respectively

$$\begin{aligned} A_b P_b + P_b A_b^T + B_b B_b^T &= 0 \\ Q_b A_b + A_b^T Q_b + C_b^T C_b &= 0 \end{aligned} \tag{1.18}$$

Now if we partition the balanced system as in (1.19), then the reduced-order system obtained via direct truncation is defined by (1.20) with transfer function given by (1.21).

$$\begin{gathered} A_b = \begin{bmatrix} A_{11} & A_{12} \\ A_{21} & A_{22} \end{bmatrix}, B_b = \begin{bmatrix} B_{11} \\ B_{22} \end{bmatrix}, C_b = [C_{11} \quad C_{22}], D_b = D \\ \Sigma = \begin{bmatrix} \Sigma_1 & 0 \\ 0 & \Sigma_2 \end{bmatrix} \\ \Sigma_1 = diag(\sigma_1, \dots, \sigma_r), \qquad \Sigma_2 = diag(\sigma_{r+1}, \dots, \sigma_n) \end{gathered} \tag{1.19}$$

$$\begin{aligned} \dot{x}_1(t) &= A_{11} x_1(t) + B_{11} u(t) \\ y(t) &= C_{11} x_1(t) + D u(t) \end{aligned} \tag{1.20}$$

$$G_{11}(s) = C_{11}(sI - A_{11})^{-1} B_{11} + D \tag{1.21}$$

The reduced-order system is also balanced and asymptotically stable [11] and it has been shown that its H_∞ norm satisfies [4]

$$\|G(s) - G_{11}(s)\|_\infty \leq 2(\sigma_{r+1} + \sigma_{r+2} + \cdots + \sigma_n) \tag{1.22}$$

The residualized reduced-order system given in Liu and Anderson [1] has the following form

$$\begin{aligned} \dot{x}_1(t) &= A_r x_1(t) + B_r u(t) \\ y(t) &= C_r x_1(t) + D_r u(t) \end{aligned} \tag{1.23}$$

where

$$\begin{aligned} A_r &:= A_{11} - A_{12} A_{22}^{-1} A_{21} \\ B_r &:= B_{11} - A_{12} A_{22}^{-1} B_{22} \\ C_r &:= C_{11} - C_{22} A_{22}^{-1} A_{21} \\ D_r &:= D - C_{22} A_{22}^{-1} B_{22} \end{aligned} \tag{1.24}$$

It has been shown that the transfer function of the residualized system is

$$G_r(s) = C_r(sI - A_r)^{-1}B_r + D_r \tag{1.25}$$

and its H_∞ norm satisfies

$$\|G(s) - G_r(s)\|_\infty \leq 2(\sigma_{r+1} + \sigma_{r+2} + \cdots + \sigma_n) \tag{1.26}$$

1.6 Introduction to Singularly Perturbed Systems

We now consider a linear time-invariant singularly perturbed system given by

$$\begin{aligned} \dot{x}_1(t) &= A_{11}x_1(t) + A_{12}x_2(t) + B_{11}u(t) \\ \varepsilon\dot{x}_2(t) &= A_{21}x_1(t) + A_{22}x_2(t) + B_{22}u(t) \\ y(t) &= C_{11}x_1(t) + C_{22}x_2(t) + Du(t) \end{aligned} \tag{1.27}$$

In (1.27), ε ($0 < \varepsilon \ll 1$) is a small positive singular perturbation parameter [6]. Matrices A_{11} and A_{22} are of dimensions $r \times r$ and $(n-r) \times (n-r)$ respectively. It is assumed that matrix A_{22} is invertible [2], [4], and [39].

It is well known (Kokotovic and Khalil [39]) that for sufficiently small ε, the dynamics of the system in (1.27) can be approximated by the dynamics of lower-dimensional slow and fast subsystems. This technique has two main advantages:

- We are dealing with two lower-dimensional systems
- The perturbation parameter disappears in the slow and fast subsystems thus avoiding possible numerical ill-conditioning.

The *slow* subsystem is represented by [4]

$$\begin{aligned} \dot{x}_1(t) &= A_0x_1(t) + B_0u(t) \\ x_2(t) &= -A_{22}^{-1}A_{21}x_1(t) - A_{22}^{-1}B_{22}u(t) \\ y(t) &= C_0x_1(t) + D_0u(t) \end{aligned} \tag{1.28}$$

The second equation in (1.28) is obtained by solving the second equation of the quasi steady state system of (1.27). The matrices A_o, B_o, C_o and D_o are defined in (1.29).

$$
\begin{aligned}
A_0 &:= A_{11} - A_{12}A_{22}^{-1}A_{21} \\
B_0 &:= B_{11} - A_{12}A_{22}^{-1}B_{22} \\
C_0 &:= C_{11} - C_{22}A_{22}^{-1}\,A_{21} \\
D_0 &:= -C_{22}A_{22}^{-1}B_{22}
\end{aligned}
\tag{1.29}
$$

The *fast* subsystem is given by

$$
\begin{aligned}
\dot{x}_2(\tau) &= A_{22}x_2(\tau) + B_{22}u(\tau) \\
y(\tau) &= C_{11}x_1(t) + Du(t)
\end{aligned}
\tag{1.30}
$$

where $\tau = \frac{t}{\varepsilon}$.

An important technique that helps determine the dynamics of a system using the slow and fast subsystems utilizes the famed Chang transformation [9]. This transformation decouples exactly linear singularly perturbed systems into slow and fast subsystems. The highlights of the Chang transformation are given below.

Let us define a linear singularly perturbed deterministic system

$$
\begin{aligned}
\dot{x}_1(t) &= A_{11}x_1(t) + A_{12}x_2(t) + B_{11}u(t) \\
\varepsilon\dot{x}_2(t) &= A_{21}x_1(t) + A_{22}x_2(t) + B_{22}u(t) \\
y(t) &= C_{11}x_1(t) + C_{22}x_2(t) + Du(t)
\end{aligned}
\tag{1.31}
$$

We can transform the system in (1.31) into pure-slow and pure-fast subsystems via the Chang transformation [9]

$$
\begin{aligned}
\dot{z}_1 &= (A_{11} - A_{12}L)z_1 + (B_{11} - HB_{22} - \varepsilon HLB_{11})u = A_s z_1 + B_s u \\
\varepsilon\dot{z}_2 &= (A_{22} + \varepsilon LA_{12})z_2 + (B_{22} + \varepsilon LB_{11})u = A_f z_2 + B_f u \\
y &= (C_{11} - C_{22}L)z_1 + (C_{22} - \varepsilon C_{22}LH + \varepsilon C_{11}H)z_2 + Du = C_s z_1 + C_f z_2 + Du
\end{aligned}
\tag{1.32}
$$

where

$$
\begin{aligned}
A_s &= A_{11} - A_{12}L, \quad & B_s &= B_{11} - HB_{22} - \varepsilon HLB_{11} \\
A_f &= A_{22} + \varepsilon LA_{12}, \quad & B_f &= C_{22} - \varepsilon C_{22}LH + \varepsilon C_{11}H \\
C_s &= C_{11} - C_{22}L, \quad & C_f &= C_{22} - \varepsilon C_{22}LH + \varepsilon C_{11}H
\end{aligned}
\tag{1.33}
$$

with

$$
\begin{bmatrix} z_1(t) \\ z_2(t) \end{bmatrix} = \begin{bmatrix} I - \varepsilon HL & -\varepsilon H \\ L & I \end{bmatrix} \begin{bmatrix} x_1(t) \\ x_2(t) \end{bmatrix} = T \begin{bmatrix} x_1(t) \\ x_2(t) \end{bmatrix}
\tag{1.34}
$$

The matrix T on the right of (1.34) is known as the similarity transformation matrix. Matrices L and H satisfy the following algebraic equations

$$\begin{aligned} A_{22}L - A_{21} - \varepsilon L(A_{11} - A_{12}L) &= 0 \\ HA_{22} - A_{12} + \varepsilon(HLA_{12} - A_{11}H + A_{12}LH) &= 0 \end{aligned} \tag{1.35}$$

A unique solution to (1.35) exists under the assumption that ε is sufficiently small and matrix A_{22} is nonsingular. There are several algorithms that can be used to solve (1.35), see for example [5], [12], and [13]. We will utilize the Newton method [5] for the iterative solution of (1.35). The algorithm, which has a quadratic rate of convergence of $O(\varepsilon^{2i})$ is outlined below.

$$\begin{aligned} D_1^{(i)}L^{(i+1)} + L^{(i+1)}D_2^{(i)} &= Q^{(i)} \\ D_1^{(i)} = A_{22} + \varepsilon L^{(i)}A_{12},\ \ D_2^{(i)} &= -\varepsilon\left(A_{11} - A_{12}L^{(i)}\right) \\ Q^{(i)} = A_{21} + \varepsilon L^{(i)}A_{12}L^{(i)},\ \ L^{(0)} &= A_{22}^{-1}A_{21} \end{aligned} \tag{1.36}$$

Once we obtained L from (1.36), we can solve (1.37) directly as a linear Sylvester equation to obtain H.

$$H^{(i+1)}D_1^{(i+1)} + D_2^{(i+1)}H^{(i+1)} = A_{12} \tag{1.37}$$

1.6.1 Decoupling the Lyapunov Differential Equation of a Singularly Perturbed System Using the Chang Transformation

In this section we will explain how to obtain a completely decoupled reduced-order differential and algebraic Lyapunov equation by using the Chang transformation.

The so-called regulator type differential Lyapunov equation is given by

$$\dot{P} = A^T P + PA + Q, \qquad P(t_0) = P_0 \tag{1.38}$$

Matrices A, P and Q have the following structure [3]

$$A = \begin{bmatrix} A_{11} & A_{12} \\ \frac{1}{\varepsilon}A_{21} & \frac{1}{\varepsilon}A_{22} \end{bmatrix}, P = \begin{bmatrix} P_{11} & \varepsilon P_{12} \\ \varepsilon P_{12}^T & \varepsilon P_{21} \end{bmatrix}, Q = \begin{bmatrix} Q_{11} & Q_{12} \\ Q_{12}^T & Q_{21} \end{bmatrix} \tag{1.39}$$

Substituting (1.39) in (1.38) we obtain

$$\begin{aligned} \dot{P}_1 &= A_1^T P_1 + P_1 A_1 + A_3^T P_2^T + P_2 A_3 + Q_1 \\ \varepsilon \dot{P}_2 &= \varepsilon A_1^T P_2 + P_1 A_2 + A_3^T P_3 + P_2 A_4 + Q_2 \\ \varepsilon \dot{P}_3 &= \varepsilon A_2^T P_2 + P_1 A_2 + A_3^T P_3 + P_2 A_4 + Q_2 \end{aligned} \tag{1.40}$$

In (1.40) variables P_2 and P_3 change quickly meanwhile P_1 is a slow variable. By looking at (1.38) and (1.39) we can tell that (1.40) is numerically ill-conditioned hence it is necessary to decouple it. We start by multiplying (1.38) by T^{-T} from the left-hand side and by T^{-1} from the right-hand side. Matrix T is the Chang transformation matrix defined in the previous section.

$$T^{-T}\dot{P}T^{-1} = T^{-T}\,A^T P T^{-1} + T^{-T}\,P A T^{-1} + T^{-T}\,Q T^{-1} \tag{1.41}$$

(1.41) can be written as

$$\dot{K} = a^T K + K a + q, \qquad K(t_0) = K_0 \tag{1.42}$$

where

$$\begin{aligned} a = TAT^{-1} &= \begin{bmatrix} A_s & 0 \\ 0 & \frac{1}{\varepsilon}A_f \end{bmatrix} \\ q = T^{-T}QT^{-1} &= \begin{bmatrix} q_1 & q_2 \\ q_2^T & q_3 \end{bmatrix} \\ K = T^{-T}PT^{-1} &= \begin{bmatrix} K_1 & \varepsilon K_2 \\ \varepsilon K_2^T & \varepsilon K_3 \end{bmatrix} \Rightarrow P = T^T K T \end{aligned} \tag{1.43}$$

Now we can partition (1.42) to obtain a completely decoupled form of (1.38) and (1.40) as

$$\begin{aligned} \dot{K}_1 &= K_1 A_s + A_s^T K_1 + q_1 \\ \varepsilon \dot{K}_2 &= K_2 A_f + A_s^T K_2 + q_2 \\ \varepsilon \dot{K}_3 &= K_3 A_f + A_f^T K_3 + q_3 \end{aligned} \tag{1.44}$$

The same derivation holds for the corresponding algebraic Lyapunov equations. Using a bar to denote the corresponding steady state quantities we have

$$\begin{aligned} 0 &= \bar{K}_1 \bar{A}_s + \bar{A}_s^T \bar{K}_1 + \bar{q}_1 \\ 0 &= \bar{K}_2 \bar{A}_f + \bar{A}_s^T \bar{K}_2 + \bar{q}_2 \\ 0 &= \bar{K}_3 \bar{A}_f + \bar{A}_f^T \bar{K}_3 + \bar{q}_3 \end{aligned} \tag{1.45}$$

In summary, either $P(t)$ or $\bar{P} = \lim_{t\to\infty} P(t)$ can be obtained exactly from the reduced-order Lyapunov equations (1.44) and (1.45) with

$$P(t) = T^T \begin{bmatrix} K_1 & \varepsilon K_2 \\ \varepsilon K_2^T & \varepsilon K_3 \end{bmatrix} T \tag{1.46}$$

or

$$\bar{P} = T^T \begin{bmatrix} \bar{K}_1 & \varepsilon \bar{K}_2 \\ \varepsilon \bar{K}_2^T & \varepsilon \bar{K}_3 \end{bmatrix} T \tag{1.47}$$

Chapter 2

2. Balanced Realization of the Linearized Fuel Cell – Reformer Model

As we stated earlier in the introduction, we will be investigating the 18th - order coupled fuel cell – natural gas reformer system in this study. We will present the 8th - order linearized model given in [33] but we will not elaborate on it. The focus will be the overall 18th - order model.

2.1 Balancing Transformation of the 8th - Order Linear Fuel Cell Model

The linearized model of the fuel cell is developed in [33]. It has the following form

$$\begin{aligned} \delta\dot{x}^{FC}(t) &= A^{FC}\delta x^{FC}(t) + B^{FC}\delta u_{blow}(t) + G_w^{FC}\delta w(t) \\ y^{FC}(t) &= C^{FC}\delta x^{FC}(t) + D^{FC}\delta u_{blow}(t) + E^{FC}\delta w(t) \end{aligned} \qquad (2.1)$$

The state $x(t)$, measurements $y(t)$, input $u(t)$, and disturbance $w(t)$ are

$$\begin{gathered} x^{FC} = [m_{o_2} \quad m_{H_2} \quad m_{N_2} \quad \omega_{cp} \quad p_{sm} \quad m_{sm} \quad m_{\omega,an} \quad p_{rm}]^T \\ y^{FC} = [W_{cp} \quad p_{sm} \quad v_{st}]^T \\ u = v_{cm} \\ w = I_{st} \end{gathered} \qquad (2.2)$$

All the corresponding matrices of model (2.1) except for the disturbance matrices (which we are not using) can be found in Table 5. The balancing transformation of this model has already been investigated in [40] and we will extend those results to the 18th order fuel cell – reformer system. The notations used in (2.2) are defined in Table 4.

Table 4: Fuel cell notation definitions

Symbol	Definition
m_{o_2}	Mass of oxygen
m_{H_2}	Mass of hydrogen
m_{N_2}	Mass of nitrogen
ω_{cp}	Compressor speed (rad/sec)
p_{sm}	Pressure of gas in supply manifold
m_{sm}	Mass of gas in supply manifold
$m_{w,an}$	Mass of water in the anode channel
p_{rm}	Pressure in the return manifold
W_{cp}	Compressor flow rate
v_{st}	Stack voltage
v_{cm}	Compressor motor input voltage
I_{st}	Stack current
u_{blo}	Air blower signal
u_{valve}	Valve blower signal

Table 5: Linearized matrices of the PEM fuel cell

A^{FC}

-6.3091	0	-10.954	0	83.7446	0	0	24.0587
0	-161.08	0	0	51.5292	0	-18.026	0
-18.786	0	-46.314	0	275.659	0	0	158.374
0	0	0	-17.351	193.937	0	0	0
1.2996	0	2.9693	0.3977	-38.702	0.1057	0	0
16.6424	0	38.0252	5.0666	-479.38	0	0	0
0	-450.39	0	0	142.208	0	-80.947	0
2.0226	0	4.6212	0	0	0	0	-51.211

B^{FC}

0
0
0
3.9467
0
0
0
0

D^{FC}

0
0
0

C^{FC}

0	0	0	5.0666	-116.45	0	0	0
0	0	0	0	1	0	0	0
12.9699	10.3253	-0.5693	0	0	0	0	0

2.2 Balancing Transformation of the 18th - Order LTI Fuel Cell – Reformer Model

To couple the fuel cell and the reformer models together we start by defining the 10th order linearized fuel processor system (reformer). The model is shown in (2.3) with $\delta u = \frac{\delta u_{blo}}{\delta u_{val}}$.

$$\begin{aligned} \delta \dot{x}^{FPS} &= A^{FPS}\delta x^{FPS} + B^{FPS}\delta u + G^{FPS}\delta w \\ y^{FPS} &= C^{FPS}\delta x^{FPS} + [D_{blo}^{FPS} \quad D_{val}^{FPS}]\delta u + E^{FPS}\delta w \end{aligned} \tag{2.3}$$

All the matrices of (2.3) are defined in Table 7. The state $x(t)$, the input $u(t)$, and disturbance $w(t)$ are respectively defined in (2.4).

$$\begin{aligned} x^{FPS} &= [T_{cpox} \quad p_{H_2}^{an} \quad p^{an} \quad p^{hex} \quad \omega_{blo} \quad p^{hds} \\ &\quad p_{CH_4}^{mix} \quad p_{air}^{mix} \quad p_{H_2}^{wrox} \quad p^{wrox}]^T \\ u &= [u_{blo} \quad u_{valve}]^T \\ w &= I_{st} \end{aligned} \tag{2.4}$$

Table 6 defines the notations of (2.4).

Table 6: Reformer notation definitions

T_{cpox}	Catalyst temperature
$p_{H_2}^{an}$	Pressure of hydrogen in the anode
p^{an}	Anode pressure
p^{hex}	Heat exchanger pressure
ω_{blo}	Speed of the blower (rad/sec)
p^{hds}	Pressure of hydro-desulfurizer
$p_{CH_4}^{mix}$	Pressure of CH_4 in the mixer
p_{air}^{mix}	Pressure of air in the mixer
$p_{H_2}^{wrox}$	Hydrogen pressure in water gas shift converter (WROX)
p^{wrox}	Total pressure in WROX

Table 7: Linearized matrices of the reformer system

A^{FPS}

-0.074	0	0	0	0	0	-3.53	1.0748	0	1E-06
0	-1.468	-25.3	0	0	0	0	0	2.5582	13.911
0	0	-156	0	0	0	0	0	0	33.586
0	0	0	-124.5	212.63	0	112.69	112.69	0	0
0	0	0	0	-3.333	0	0	0	0	0
0	0	0	0	0	-32.43	32.304	32.304	0	0
0	0	0	0	0	331.8	-344	-341	0	9.9042
0	0	0	221.97	0	0	-253.2	-254.9	0	32.526
0	0	2.0354	0	0	0	1.8309	1.214	-0.358	-3.304
0.0188	0	8.1642	0	0	0	5.6043	5.3994	0	-13.61

B^{FPS}

0	0
0	0
0	0
0	0
0.12	0
0	0.1834
0	0
0	0
0	0
0	0

D^{FPS}

0	0
0	0

C^{FPS}

1	0	0	0	0	0	0	0	0	0
0	0.994	-0.088	0	0	0	0	0	0	0

We now proceed to define the overall coupled LTI system using results from [30]. The coupled system has the following state space form

$$\begin{bmatrix} \delta\dot{x}^{FC} \\ \delta\dot{x}^{FPS} \end{bmatrix} = \begin{bmatrix} A^{FC} & 0 \\ 0 & A^{FPS} \end{bmatrix} \begin{bmatrix} \delta x^{FC} \\ \delta x^{FPS} \end{bmatrix} + \begin{bmatrix} B^{FC} & 0 \\ B_1^{FPS} & B_2^{FPS} \end{bmatrix} \begin{bmatrix} \delta u_{blo} \\ \delta u_{val} \end{bmatrix} + \begin{bmatrix} E^{FC} \\ E^{FPS} \end{bmatrix} \delta w \qquad (2.5)$$

$$\delta y = \begin{bmatrix} y^{FC} \\ y^{FPS} \end{bmatrix} = \begin{bmatrix} C^{FC} & 0 \\ 0 & C^{FPS} \end{bmatrix} \begin{bmatrix} \delta x^{FC} \\ \delta x^{FPS} \end{bmatrix} + \begin{bmatrix} D_{blo}^{FC} & 0 \\ D_{blo}^{FPS} & D_{val}^{FPS} \end{bmatrix} \begin{bmatrix} \delta u_{blo} \\ \delta u_{val} \end{bmatrix} + \begin{bmatrix} E^{FC} \\ E^{FPS} \end{bmatrix} \delta w$$

With the help of MATLAB we are able to put this MIMO system into balanced coordinates. The Hankel singular values of the balanced system are shown in Table 7.

Table 8: Hankel singular values of the full system

25.60763836134406
2.01988385423792
1.21474392320380
0.70365666238635
0.38531820753714
0.15631858030661
0.05720423543465
0.01511029257832

0.00502216085300
0.00160140766543
0.00058469735238
0.00010379403288
0.00004321862626
0.00002995901222
0.00000890678138
0.00000098707658
0.00000007729738
0.00000001121134

A graphical representation of the Hankel singular value decomposition is shown in Figure 3. By comparing these values we can see that the first six state variables are more dominant than the others (especially the first one). Hence we can infer that we can get a good approximation of the system by ignoring the non-dominant corresponding state components because they have insignificant contribution to the input-output map. In the following sections we will investigate the step and impulse responses of the reduced-order models (via direct truncation) and compare them with responses of the overall 18^{th} -order model.

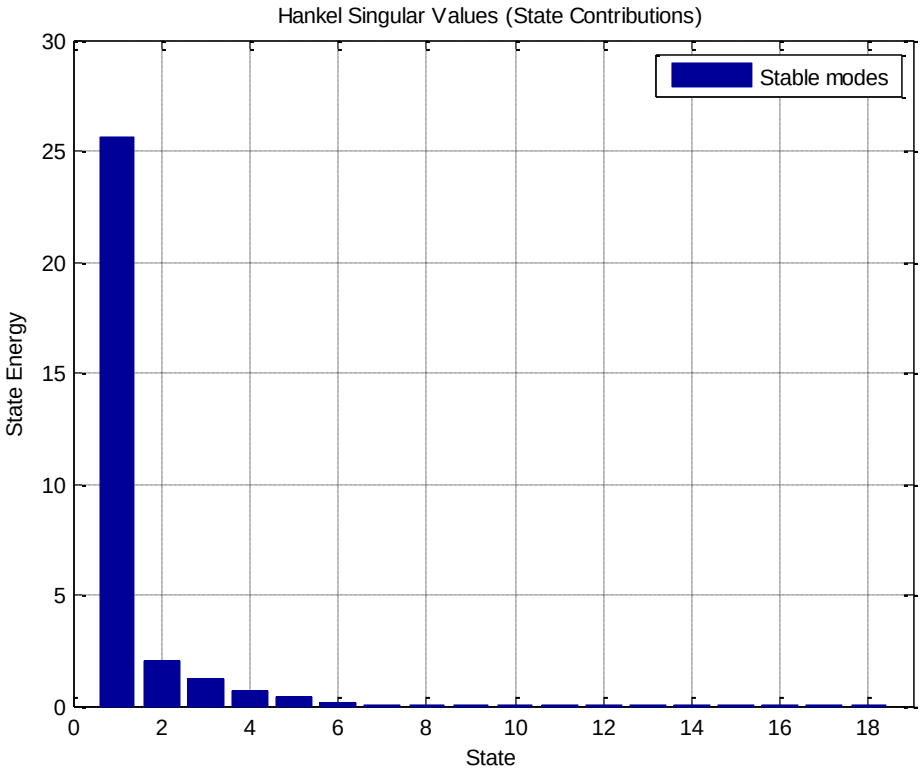

Figure 3. Hankel singular value decomposition

2.3 Step and Impulse Responses of the Reduced-Order Models via Direct Truncation

We will compare the step and impulse responses of the 18^{th} order LTI model with the reduced-order models ranging from 10^{th} to 3^{rd} - order. Since we are dealing with a MIMO model (two inputs and five outputs), ten plots are generated in total.

2.3.1 Step Response

The 18^{th} order MIMO system has two input and five outputs therefore ten step responses are generated overall. For our purposes we will only investigate the step response due to the first input and third output. That step response is shown in Figure 4.

As we can see in Figure 4, the response settles approximately after five seconds to a value of 0.712. To compare it with the reduced-order linear models we truncate the overall balanced system. The truncation ranges from a 10^{th} - order down to a 3^{rd} - order system i.e. $r = 10, \ldots, 3$. The results of the step responses are shown in Figure 5. From the plot it is clearly visible that the step response of the 10^{th} - order system is almost identical to that of the actual 18^{th} - order system. Furthermore we can see that even lower orders such as the 9^{th}, 8^{th}, and 7^{th} have a step response quite similar to that of the full order system. This indicates that order reduction of the balanced system via direct truncation (even down to 7^{th} - order in our case) gives a good approximation of the actual 18^{th} - order linear fuel cell – reformer model.

Next we investigate the impulse response of the full order and reduced-order systems.

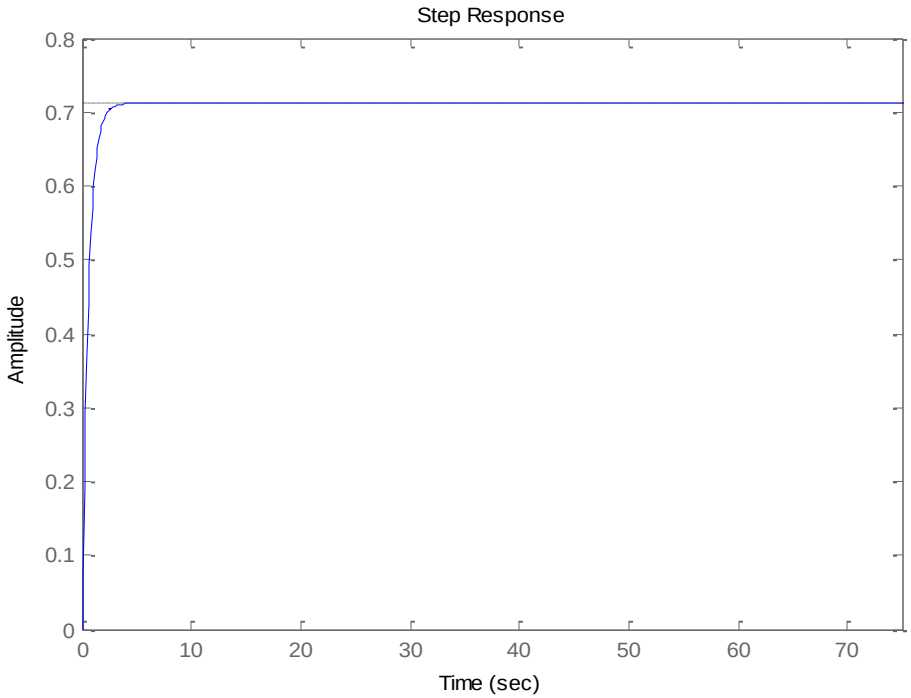

Figure 4. Step response of 18th order LTI model due to Input 1 and Output 3

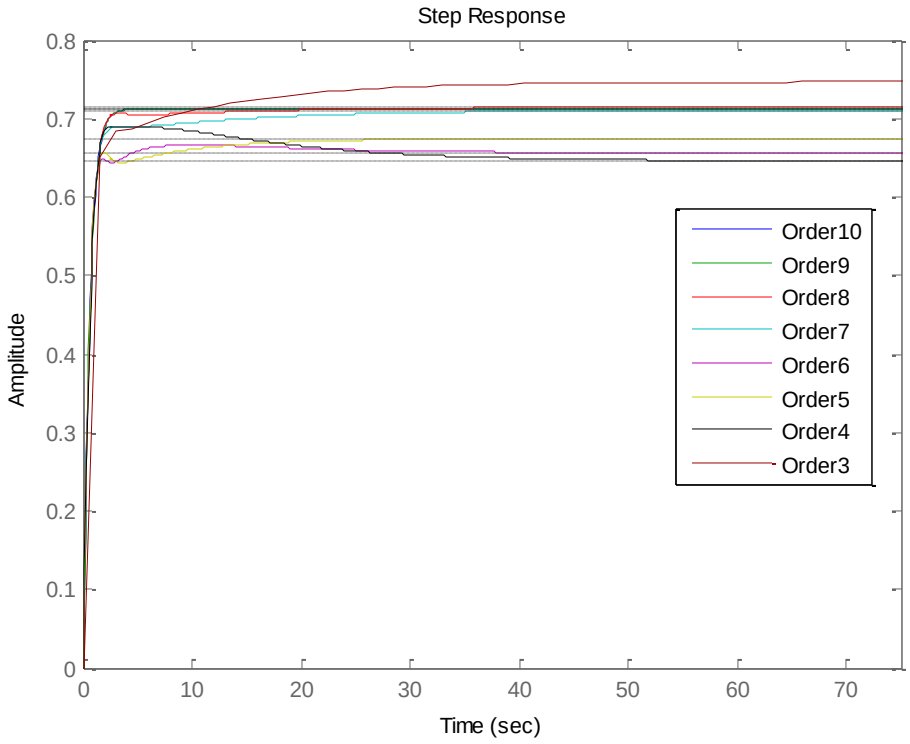

Figure 5. Step response of reduced-order LTI models due to Input 1 and Output 3

2.3.2 Impulse Response

For the impulse response we will also consider the response given by the first input and the third output. The plot generated with the help of MATLAB is shown in Figure 6. The plots of the reduced-order systems ($r = 10, \dots, 3$) via direct truncation are depicted in Figure 7. Figure 8 is a zoomed version of Figure 7. We can clearly see that the impulse response of the 4^{th} or even 3^{rd} - order system is similar to that of the full order system shown in Figure 6. Hence we can conclude that the individual reduced-order systems obtained through direct truncation of the balanced system give a very good approximation of the system's impulse response. On the other hand, the system's step response approximation from the individual step responses of the reduced-order systems (ranging from 6^{th} to 3^{rd} in our case) displays a steady state error. This happens because

the original system and the reduced-order systems have different DC gains. In the following section we will present a technique which corrects this discrepancy.

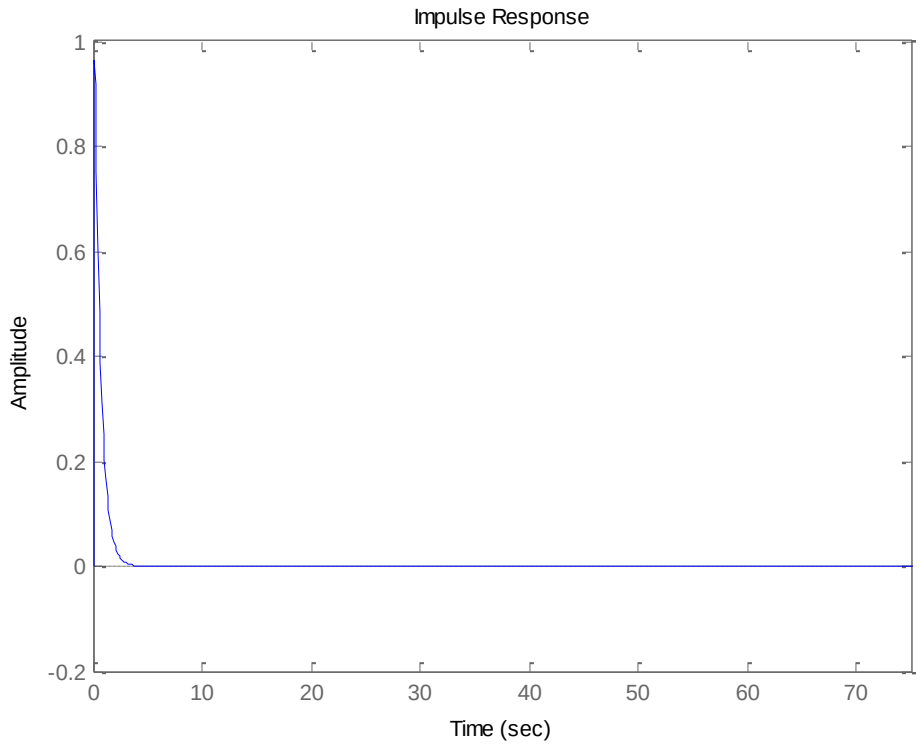

Figure 6. Impulse response of 18th order LTI model due to Input 1 and Output 3

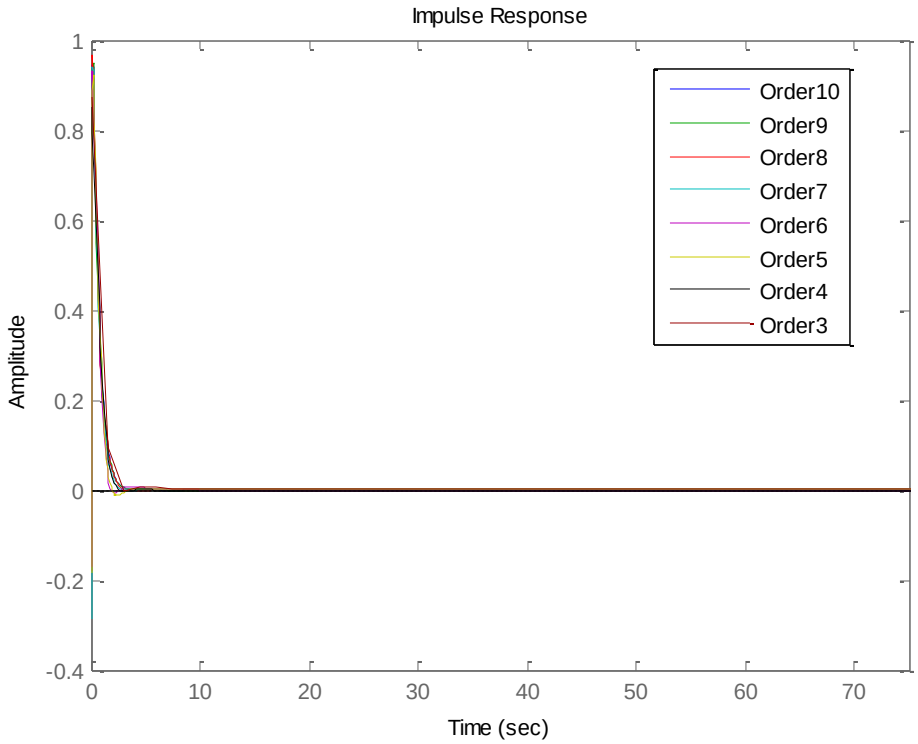

Figure 7. Impulse response of reduced-order LTI models due to Input 1 and Output 3

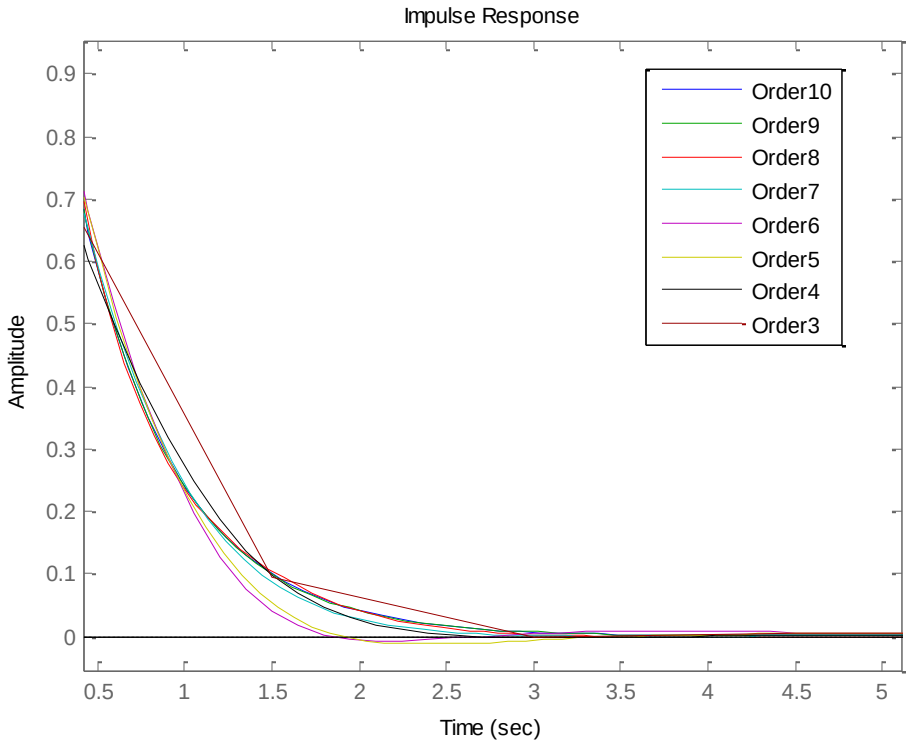

Figure 8. Impulse response of reduced-order LTI models due to Input 1 and Output 3 (zoomed)

2.4 Step and Impulse Responses of the Reduced-Order Models via Residualization Method

The balancing residualization technique presented in Section 1.4 is known to reduce the response steady state error to zero. We will obtain the step and impulse responses of the reduced-order systems using the residualization technique and then compare them with the results we obtained in the previous section.

2.4.1 Step Response

Here we consider the step responses of the reduced-order models ranging from 10^{th} order down to 3^{rd} order i.e. $r = 10, \ldots, 3$. The plots obtained for the step responses using the residualization technique are shown in Figure 9 and Figure 10 (zoomed version of Figure 9). As we can see, all the plots are quite identical to the step response of the overall 18^{th} order model from the first input and the third output shown in Figure 4. This agrees with the claim that we made earlier that the residualization technique gives a better approximation of the system's step response than the direct truncation method. This is clearly visible if we were to compare Figure 5 with Figure 9.

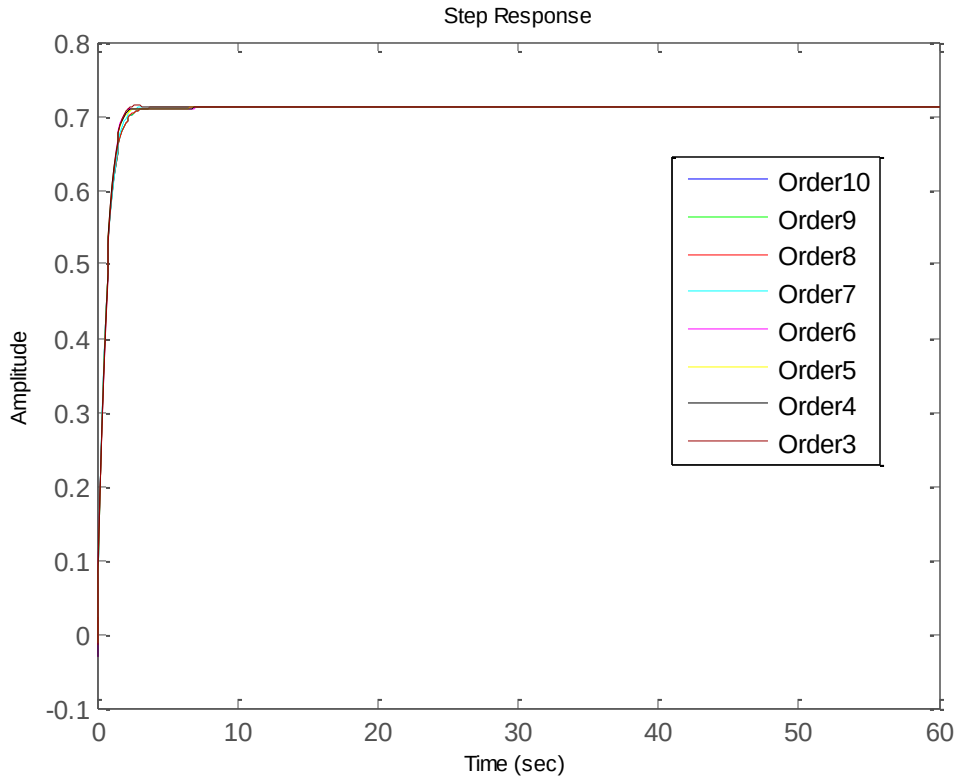

Figure 9. Step response of reduced-order LTI models due to Input 1 and Output 3

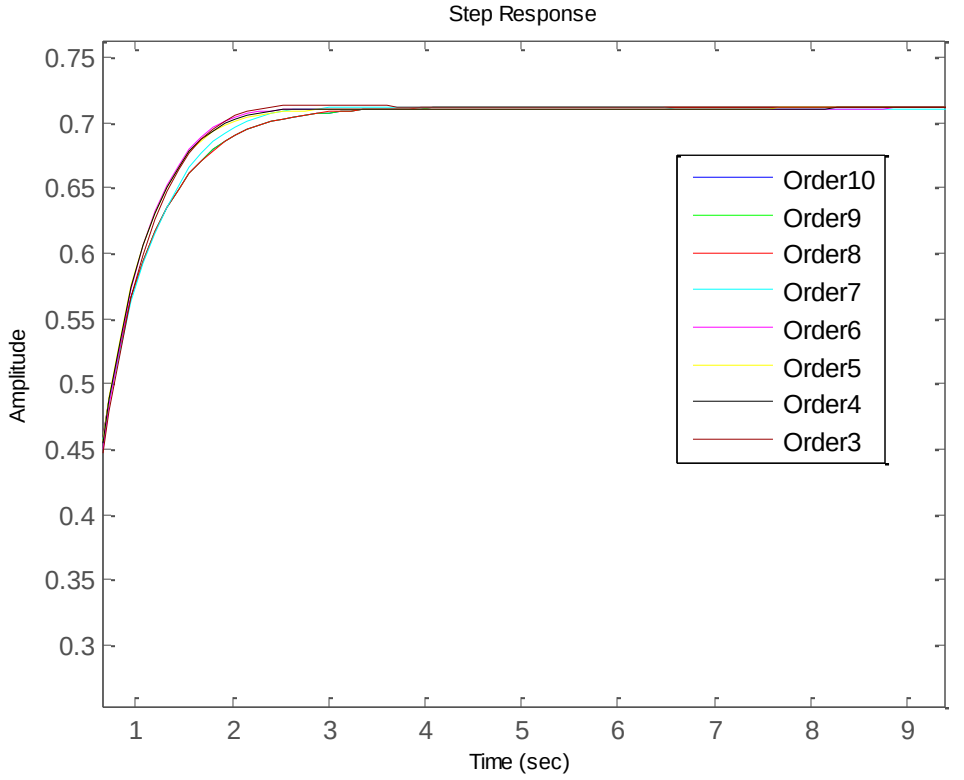

Figure 10. Step response of reduced-order models due to Input 1 and Output 3 (zoomed)

2.4.2 Impulse Response

Figure 11 and Figure 12 (zoomed version of Figure 11) show the impulse responses for each of the reduced-order systems (order 10 to 3) obtained using the balancing residualization technique. By comparing it to Figure 6 we can see that the impulse response of the individual reduced-order systems is a very good approximation of the system's impulse response just like we concluded using the direct truncation technique.

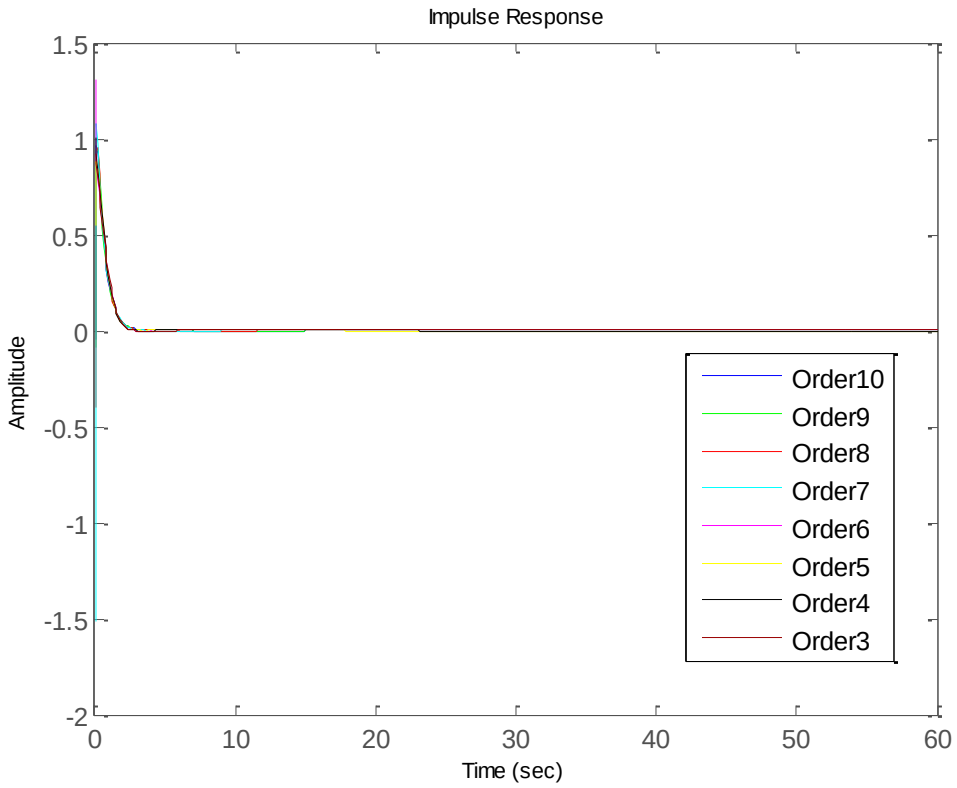

Figure 11. Impulse responses via balancing residualization

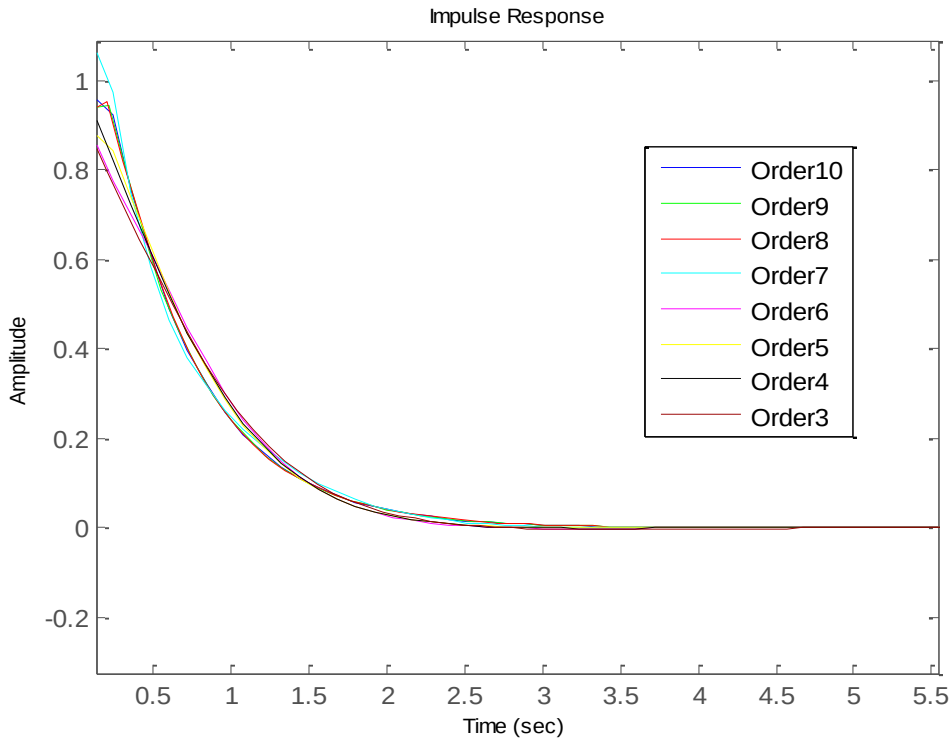

Figure 12. Impulse responses via balancing residualization (zoomed)

2.5 Frequency Behavior of Reduced-Order Models

Now we consider the frequency errors of the above order reductions. According to Anderson and Liu [20], the residualization method has very good approximation errors at low frequencies meanwhile the direct truncation technique is the opposite i.e. it displays very good approximation errors at high frequencies. Figure 13 shows the frequency response of the full order system as well as three reduced-order systems (10^{th}, 9^{th}, and 8^{th}) using both techniques, direct truncation (DT) and residualization (RES). As we can see from the figure, at higher frequencies ($\omega > 100$), the direct truncation method gives a better approximation than the residualization method.

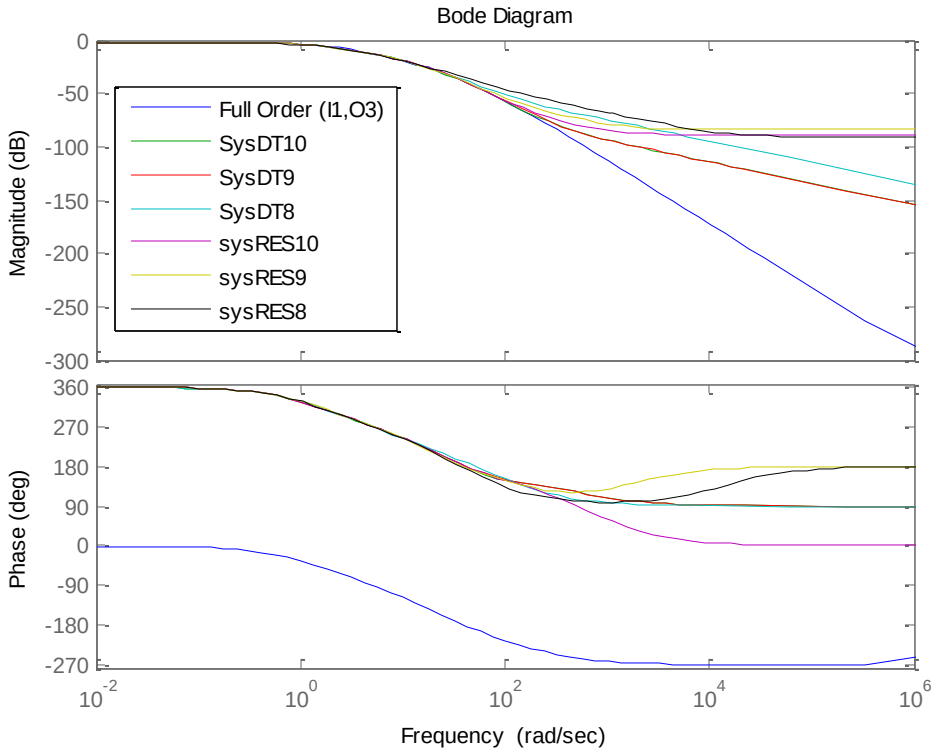

Figure 13. Frequency response of full and reduced-order systems

2.6 Optimal Performance Criterion and Riccati Equation in Balanced Coordinates

In this section we will investigate how the continuous-time Riccati equation (CARE) and the optimal performance criterion would change if we were to go to balanced coordinates.

For a system such as the one given in (1.12), the performance criterion to be optimized is given in (2.6).

$$J = \int_0^\infty [x^T(t)Qx(t) + u^T(t)Ru(t)]dt,\ Q = Q^T \geq 0, R = R^T \geq 0 \qquad (2.6)$$

We assume that full-state feedback is available and define static feedback control in the following way

$$u\big(x(t)\big) = -F_{opt}x(t) \qquad (2.7)$$

where F_{opt} is given by

$$F_{opt} = R^{-1}B^T P \tag{2.8}$$

and P is the solution of the CARE given in (2.9) [7]

$$A^T P + PA + Q - PBR^{-1}B^T P = 0 \tag{2.9}$$

Under balanced coordinates matrix P and the CARE become

$$P = T^T P_b T \rightarrow P_b = T^{-T} P T^{-1} \tag{2.10}$$

$$A_b^T P_b + P_b A_b + Q_b - P_b B_b R^{-1} B_b^T P_b = 0 \tag{2.11}$$

Now if we substitute the balanced matrices from (1.16) and P_b from (2.10) in (2.11), we obtain the following

$$T^{-T}A^T P T^{-1} + T^{-T} P A^T T^{-1} + T^{-T} Q T^{-1} - T^{-T} P B R^{-1} B^T P T^{-1} = 0 \tag{2.12}$$

Multiplying the left-hand side of (2.12) with $T^T$and its right-hand side with T the equation simplifies to the algebraic Riccati equation given in (2.9). Hence we conclude that during a similarity transformation, the CARE is preserved just like the system's eigenvalues and transfer function.

In a similar fashion we can investigate if the optimal performance criterion in balanced coordinates given in (2.13) is equivalent to the optimal performance criterion.

$$J_{b,opt} = \frac{1}{2} x_b^T(0) \left\{ \int_0^\infty e^{(A_b - B_b F_{b,opt})^T t} (Q_b + F_{b,opt}^T R_b F_{b,opt}) e^{(A_b - B_b F_{b,opt})t} dt \right\} x_b(0) \tag{2.13}$$

It can be shown that after some algebra, the integral in (2.13) is the solution of the following algebraic Lyapunov equation

$$(A_b - B_b F_{b,opt})^T P_b + P_b \left(A_b - B_b F_{b,opt}\right) + Q_b + F_{b,opt}^T F_{b,opt} = 0 \tag{2.14}$$

The solution of Equation (2.14) can be used to evaluate the optimal performance criterion given in Equation (2.15).

$$J_{b,opt} = \frac{1}{2} x_b^T(0) P_b x_b(0) \tag{2.15}$$

Substituting $x_b(t)$ and P_b in (2.15) we obtain

$$J_{b,opt} = \frac{1}{2} x^T(0) T^T T^{-T} P T^{-1} T x(0) \tag{2.16}$$

which after simplification becomes

$$J_{b,opt} = \frac{1}{2} x^T(0) P x(0) = J_{opt} \tag{2.17}$$

Hence by looking at (2.17) we conclude that the optimal performance criterion is persevered during the similarity transformation.

2.6.1 Suboptimal Performance Criterion

For a reduced-order system, the suboptimal feedback controller is given by [22], [23]

$$u_{sub}\big(x_b(t)\big) = -F_{sub} x_b(t) \tag{2.18}$$

Following the same steps as we did with the optimal performance criterion

$$J_{b,sub} = \frac{1}{2} x_b^T(0) P_{sub} x_b(0) \tag{2.19}$$

The suboptimal gain F_{sub} is obtained by using the optimal gain F_{opt} and padding it with zeros, starting with the last entry and gradually reducing the number of feedback loops.

$$F_{sub}^{1\times n} = \begin{bmatrix} F_{opt}^{1\times r} & 0^{1\times(n-r)} \end{bmatrix} \tag{2.20}$$

Table 8 shows the simulation results obtained for the balanced full-order system. The weighted matrix is defined as $Q := 100 C^T C$ [40].

Table 9: Suboptimality with r-feedback loops

r	J suboptimal
1	296.12
2	241.54
3	**-1287.8**
4	294.67
5	172.42
6	168.55
7	168.52
8	168.51
9	168.12
10	168.12
11	168.12
12	168.12
13	168.12
14	168.12
15	168.12
16	168.12
17	168.12
18 = n	168.12 = J optimal

Table 9 shows that the suboptimal performance criterion when the system's order is reduced from the 17^{th} to the 9^{th} order is exactly the same as the optimal performance criterion of the full-order system. Even the result of a reduction down to $r = 5$ shows only a 2.5% difference between the suboptimal performance criterion and the optimal performance criterion of the full system. We can also see from Table 8 for $r = 3$ the algorithm is not feasible. For $r = 2$ and $r = 1$ the suboptimal performance criterion looses monotonicity.

Chapter 3

3. Investigation of the Singularly Perturbed Models

In this chapter we will study the balanced realizations of a linear singularly perturbed system. We will utilize the technique used in Shahruz and Behtash [3] to find the approximate balancing transformation for the full system by computing the balancing transformations for the slow and fast subsystems. Next we will make use of the Chang transformation to find the exact balancing transformation of the full system and improve the results of Shahruz and Behtash [3].

3.1 Balancing Transformation Approximation via Shahruz and Behtash Technique

The singularly perturbed system has the form given in (1.27). To determine the perturbation parameter ε we separate the system into a slow and a fast subsystem.

The small perturbation parameter $\varepsilon > 0$ in our case is the ratio of the fastest eigenvalues of the slow subsystem with the slowest eigenvalue of the fast subsystem. For example, if an asymptotically stable system with real eigenvalues $-\lambda_n, -\lambda_{n+1}, -\lambda_{n+2}, \dots, -\lambda_1$ where $-\lambda_n < -\lambda_{n+1} < \dots < \lambda_1$ is partitioned into a fast subsystem with eigenvalues $-\lambda_n, -\lambda_{n+1}, \dots, -\lambda_m$ and a slow subsystem with eigenvalues $-\lambda_{m+1}, -\lambda_{m+2}, \dots, -\lambda_r$, then the singular perturbation parameter ε is

$$\varepsilon = \frac{-\lambda_{m+1}}{-\lambda_m} \tag{3.1}$$

The eigenvalues of our system (PEMFC - Reformer) are given in Table 9.

Table 10: Eigenvalues of the full order system

System's eigenvalues
-660.68
-219.63
-157.9
-89.485
-89.137
-46.177
-22.404
-18.258
-12.169
-3.333
-2.9151
-2.771 + 0.5473i
-2.771 - 0.5473i
-1.6473
-1.468
-1.4038
-0.358
-0.086154

This table clearly indicates the presence of multiple time scales in the system. For example for $n_s = 5$, we have $\varepsilon \approx 1.64/2.77 \approx 0.6$ and for $n_s = 9$, we have $\varepsilon \approx 3.33/12.17 \approx 0.27$.

Before we proceed any further, it is important to put the overall system in singularly perturbed form. A method to convert the system from implicit to explicit singularly perturbed form is detailed next.

3.1.1 Implicit to Explicit Singularly Perturbed Linear Systems

The explicit singularly perturbed linear system is represented by

$$\begin{aligned} \dot{x}_1(t) &= A_{11}x_1(t) + A_{12}x_2(t) \\ \varepsilon\dot{x}_2(t) &= A_{21}x_1(t) + A_{22}x_2(t) \end{aligned} \tag{3.2}$$

where $x_1 \in \mathbb{R}^{n_1}$ stands for slow state variables and $x_2 \in \mathbb{R}^{n_2}$ stands for fast state variables. In addition, it is assumed that A_{22} is nonsingular ($\det(A_{22}) \neq 0$). Note that if A_{22} is singular then $x_2(t)$ contains also some slow variables and they have to be moved to the slow subsystem which will increase the dimensions of the slow variables above n_1 and reduce the dimensions of fast variables below n_2.

By letting $\tau = t/\varepsilon$ the linear singularly perturbed system in (3.2) can be written in the fast time scale representation as

$$\begin{aligned} \dot{x}_1(\tau) &= \varepsilon A_{11} x_1(\tau) + \varepsilon A_{12} x_2(\tau) \\ \dot{x}_2(\tau) &= A_{21} x_1(\tau) + A_{22} x_2(\tau) \end{aligned} \tag{3.3}$$

or

$$\frac{dx(\tau)}{d\tau} = A(\varepsilon) x(\tau) \tag{3.4}$$

where

$$A(\varepsilon) = \begin{bmatrix} \varepsilon A_{11} & \varepsilon A_{12} \\ A_{21} & A_{22} \end{bmatrix} \tag{3.5}$$

It can be observed that elements in the top row of $A(\varepsilon)$ are $O(\varepsilon)$. It can be concluded that in the fast-time scale representation [39]

$$\frac{dx_1(\tau)}{d\tau} = O(\varepsilon) \tag{3.6}$$

$$\frac{dx_2(\tau)}{d\tau} = O(1) \tag{3.7}$$

If we have a singularly perturbed system in an implicit form (this can be detected by finding the eigenvalues and observing that they are clustered into two disjoint groups) represented in the slow time scale as

$$\frac{dx(t)}{dt} = A(\varepsilon)x(t) \tag{3.8}$$

The eigenvalues of $A(\varepsilon)$ are clustered in two groups, slow ($\lambda_s(A(\varepsilon))$) which are $O(1)$ and fast ($\lambda_f(A(\varepsilon))$), which are $O(1/\varepsilon)$. The matrix $A(\varepsilon)$ has also some large elements (whose rows correspond to $\lambda_f(A(\varepsilon))$) and some small elements (whose rows correspond to $\lambda_s(A(\varepsilon))$). Let us put the above equation in the fast time scale representation by multiplying both sides by ε [39]

$$\varepsilon\frac{dx(t)}{dt} = \varepsilon A(\varepsilon)z(t) = \frac{dz(\tau)}{d\tau} = F(\varepsilon)z(\tau) \tag{3.9}$$

Apparently, $\lambda_s(\varepsilon A(\varepsilon))$ are $\lambda_s\big(\varepsilon A(\varepsilon)\big) \cup \lambda_f(\varepsilon A(\varepsilon))$ with $\lambda_s\big(\varepsilon A(\varepsilon)\big) = O(\varepsilon)$ and $\lambda_f\big(\varepsilon A(\varepsilon)\big) = O(1)$.

The algorithm for converting a singularly perturbed linear system to explicit form is as follows

Step 1: Form $F(\varepsilon)$ as

$$F(\varepsilon) = \varepsilon A(\varepsilon) \tag{3.10}$$

Step 2: Form $F(\varepsilon) = F_0 + \varepsilon F_1(\varepsilon)$ with $rank\{F_0\} = n_2$ (number of fast modes). As a matter of fact set all $O(\varepsilon)$ elements (less than some prespecified small number) to zero.

Step 3: Form matrix Q using n_2 linearly independent rows of F_0. Then

$$\eta = Qz \tag{3.11}$$

is the fast variable.

Step 4: Find the left null space of F_0

$$PF_0 = 0 \text{ or } F_0^T P^T = 0 \tag{3.12}$$

then the slow variable is

$$x = Pz \tag{3.13}$$

Step 5: Form the similarity transformation

$$T = \begin{bmatrix} P \\ Q \end{bmatrix} \tag{3.14}$$

then

$$TA(\varepsilon)T^{-1} = T\frac{F(\varepsilon)}{\varepsilon}T^{-1} = \begin{bmatrix} A_{11} & A_{12} \\ A_{21} & \frac{1}{\varepsilon}A_{22} \end{bmatrix} \tag{3.15}$$

or

$$\begin{aligned} \dot{x}(t) &= A_{11}x_1(t) + A_{12}x_2(t) \\ \varepsilon\dot{\eta}(t) &= \varepsilon A_{21}x_1(t) + A_{22}x_2(t) \end{aligned} \tag{3.16}$$

Since fuel cell models have multiple time-scale eigenvalues (singularly perturbed) we can use the above procedure to put them in the standard singularly perturbed form.

3.1.2 Gramians of Singularly Perturbed Systems and the method of [3]

Here we study the relation between the controllability and observability gramians of the full singularly perturbed linear system defined in (1.27) and also in (3.2) and gramians of the slow and fast subsystems defined in (1.28) and (1.30) respectively.

For the system defined in (1.27), we have the system of matrices

$$A = \begin{bmatrix} A_{11} & A_{12} \\ \frac{1}{\varepsilon}A_{21} & \frac{1}{\varepsilon}A_{22} \end{bmatrix}, B = \begin{bmatrix} B_{11} \\ \frac{1}{\varepsilon}B_{22} \end{bmatrix}, C = [C_{11} \quad C_{22}] \tag{3.17}$$

The controllability gramian can be obtained from

$$AP + PA^T + BB^T = 0 \tag{3.18}$$

The symmetric matrix P which is the solution of the algebraic Lyapunov equation is unique, positive definite and appropriately partitioned as [2], [10], [39]

$$P = \begin{bmatrix} P_{11} & P_{12} \\ P_{12}^T & \frac{1}{\varepsilon} P_{22} \end{bmatrix} \tag{3.19}$$

where matrices $P_{11} = P_{11}^T$, $P_{22} = P_{22}^T$, and P_{12} are of dimensions $m \times m$, $n \times n$, and $m \times n$ respectively. Furthermore it can be shown that [3],

$$\begin{aligned} P_{11} &= \bar{P}_{11} + O(\varepsilon) \\ P_{12} &= \bar{P}_{12} + O(\varepsilon) \\ P_{22} &= \bar{P}_{22} + O(\varepsilon) \end{aligned} \tag{3.20}$$

In (3.20) matrices $\overline{P}_{11} = \bar{P}_{11}^T \in \mathbb{R}^{m \times m}$, $\overline{P}_{22} = \bar{P}_{22}^T \in \mathbb{R}^{n \times n}$ and $\bar{P}_{12} \in \mathbb{R}^{m \times n}$ satisfy the following algebraic equations [3]

$$\begin{aligned} A_0 \overline{P}_{11} + \bar{P}_{11} A_0^T + B_0 B_0^T &= 0 \\ A_{22} \overline{P}_{22} + \overline{P}_{22} A_{22}^T + B_{22} B_{22}^T &= 0 \\ \bar{P}_{12}^T = -A_{22}^{-1} (\overline{P}_{22} A_{12}^T + A_{21} \overline{P}_{11} + B_{22} B_{11}^T) & \end{aligned} \tag{3.21}$$

where matrices A_0 and B_0 are given in (1.29). Matrices $\overline{P}_{11}$ and $\overline{P}_{22}$ are the approximate controllability gramians of the slow and fast subsystems respectively.

Substituting P_{11}, P_{12} and P_{22} from (3.20) into (3.19) we obtain

$$P = \begin{bmatrix} \overline{P}_{11} & \bar{P}_{12} \\ \bar{P}_{12}^T & \frac{1}{\varepsilon} \overline{P}_{22} \end{bmatrix} + \begin{bmatrix} O(\varepsilon) & O(\varepsilon) \\ O(\varepsilon) & O(1) \end{bmatrix} \tag{3.22}$$

For sufficiently small ε, the first matrix on the right-hand side of (3.22) is an approximate controllability gramian of the full system [3].

In a similar fashion we can obtain the approximate observability gramian for the full system. The observability gramian can be obtained from the following Lyapunov algebraic equation

$$QA + A^T Q + C^T C = 0 \tag{3.23}$$

With Q being appropriately partitioned as

$$Q = \begin{bmatrix} Q_{11} & \varepsilon Q_{12} \\ \varepsilon Q_{12}^T & \varepsilon Q_{22} \end{bmatrix} \tag{3.24}$$

and with the following property

$$\begin{aligned} Q_{11} &= \bar{Q}_{11} + O(\varepsilon) \\ Q_{12} &= \bar{Q}_{12} + O(\varepsilon) \\ Q_{22} &= \bar{Q}_{22} + O(\varepsilon) \end{aligned} \tag{3.25}$$

After substituting (3.25) into (3.24) we obtain

$$Q = \begin{bmatrix} \bar{Q}_{11} & \varepsilon \bar{Q}_{12} \\ \varepsilon \bar{Q}_{12}^T & \varepsilon\, \bar{Q}_{22} \end{bmatrix} + \begin{bmatrix} O(\varepsilon) & O(\varepsilon^2) \\ O(\varepsilon^2) & O(\varepsilon^2) \end{bmatrix} \tag{3.26}$$

where $\bar{Q}_{ij}$ satisfy the following

$$\begin{aligned} \bar{Q}_{11} A_o + A_o^T \bar{Q}_{11} + C_o^T C_o &= 0 \\ \bar{Q}_{22} A_{22} + A_{22}^T\, \bar{Q}_{22} + C_{22}^T C_{22} &= 0 \\ \bar{Q}_{12} = -(A_{21}^T \bar{Q}_{22} + \bar{Q}_{11} A_{12} + C_{11}^T C_{22}) A_{22}^{-1} & \end{aligned} \tag{3.27}$$

and where C_o is defined in (1.29).

Likewise, for sufficiently small ε, the first term in the right-hand side of (3.26) is an approximate observability gramian for the full system. Furthermore for the system in balanced coordinates we can find its Hankel singular values the following way

$$\sigma_i^2 = \lambda_i(PQ) \tag{3.28}$$

The product of the gramian (using (3.22) and (3.26)) is

$$PQ = \begin{bmatrix} \bar{P}_{11}\bar{Q}_{11} & 0 \\ \bar{P}_{12}^T \bar{Q}_{11} + \bar{P}_{22}\bar{Q}_{12}^T & \bar{P}_{22}\bar{Q}_{22} \end{bmatrix} + \begin{bmatrix} O(\varepsilon) & O(\varepsilon) \\ O(\varepsilon) & O(\varepsilon) \end{bmatrix} \tag{3.29}$$

Then

$$\sigma_i^2 = \lambda_i(PQ) = \lambda_i(\bar{P}_{11}\bar{Q}_{11}) \cup \lambda_i(\bar{P}_{22}\bar{Q}_{22}) + O(\varepsilon) \tag{3.30}$$

It is important to emphasize that the Hankel singular values obtained from (3.30) will only be an approximation since the technique omits the $O(\varepsilon)$ terms, which is in fact the method of [3].

Comment 1: From (3.22) and (3.26) we see that the controllability and observability gramians of the original singularly perturbed system are

$$P = \begin{bmatrix} O(1) & O(1) \\ O(1) & O(1/\varepsilon) \end{bmatrix}, Q = \begin{bmatrix} O(1) & O(\varepsilon) \\ O(\varepsilon) & O(\varepsilon) \end{bmatrix} \tag{3.31}$$

which indicates that in the original coordinates the controllability and observability measures of the slow subsystem are both $O(1)$, that is $P_{11} = O(1)$, $Q_{11} = O(1)$. However, the fast subsystem is strongly controllable ($P_{22} = O(1/\varepsilon)$) and weakly observable ($Q_{22} = O(\varepsilon)$) in the original coordinates.

The order-reduction technique based on singular perturbation (using only the slow subsystem) will neglect some dominant fast modes whose controllability measure is $O(1/\varepsilon)$. Hence the order-reduction based on system balancing seems to be more general than the order-reduction technique based on singular perturbations.

Comment 2: Another observation is that the order-reduction technique of singularly perturbed linear systems is completely based on matrices A and B (which carry only information about the system controllability) and does not take into the account the observability of the system that is

$$\begin{matrix} \dot{x}_1 = A_{11}x_1 + A_{12}x_2 + B_1u \\ \varepsilon\dot{x}_1 = A_{21}x_1 + A_{22}x_2 + B_2u \end{matrix} \Longrightarrow \begin{matrix} \dot{x}_s = A_sx_s + B_su \\ \varepsilon\dot{x}_f = A_fx_f + B_fu \end{matrix} \tag{3.32}$$

3.1.3 Computation of the Approximate Balancing Transformation of [3]

An approximate balancing transformation for the full system can be determined by computing the approximate balancing transformations for the slow and fast subsystems as was determined in [3]. We let T_0 and T_2, denote the transformation matrices for the approximate slow and fast subsystems respectively. T_0 and T_2 can be computed using the algorithm given in [36], applied respectively to

$$\begin{aligned} \dot{x}_1 &= A_0 x_1 + B_0 u, \quad & y_1 &= C_0 x_1 + D_0 u \\ \varepsilon \dot{x}_2 &= A_{22} x_2 + B_2 u, \quad & y_2 &= C_2 x_2 \end{aligned} \tag{3.33}$$

producing

$$\begin{aligned} \tilde{P}_{11} &:= T_0^{-1} \overline{P}_{11} T_0^{-T} = \tilde{Q}_{11} := T_0^T \overline{Q}_{11} T_0 = \Sigma_0 \\ \tilde{P}_{22} &:= T_2^{-1} \overline{P}_{22} T_2^{-T} = \tilde{Q}_{22} := T_2^T \overline{Q}_{22} T_2 = \Sigma_2 \end{aligned} \tag{3.34}$$

Note that $\Sigma_0 = \Sigma_s + O(\varepsilon)$ and $\Sigma_2 = \Sigma_f + O(\varepsilon)$.

In Equation (3.34) $\overline{P}_{11}$ and $\overline{P}_{22}$ are the approximate controllability gramians of the slow and fast subsystems respectively defined in (3.22). $\overline{Q}_{11}$ and $\overline{Q}_{22}$ represent the approximate observability gramians of the slow and fast subsystems respectively defined in (3.26).

The approximate system's balancing transformation matrix is defined in [5] using the balancing transformation matrices of the slow and fast subsystems as

$$\hat{T} = \begin{bmatrix} T_0 & 0 \\ 0 & \frac{1}{\varepsilon} T_2 \end{bmatrix} \tag{3.35}$$

Using the approximate controllability and observability gramians given in (3.22) and (3.26), we can compute $\hat{T}^{-1} \bar{P} \hat{T}^{-T}$ and $\hat{T}^T \bar{Q} \hat{T}$.

$$\hat{T}^{-1}\bar{P}\hat{T}^{-T} = \begin{bmatrix}\Sigma_0 & 0\\ 0 & \Sigma_2\end{bmatrix} = \begin{bmatrix}\Sigma_s & 0\\ 0 & \Sigma_f\end{bmatrix} + \begin{bmatrix}O(\varepsilon) & O(\varepsilon^{1/2})\\ O(\varepsilon^{1/2}) & O(\varepsilon)\end{bmatrix} \tag{3.36}$$

$$\hat{T}^{T}\bar{Q}\hat{T} = \begin{bmatrix}\Sigma_0 & 0\\ 0 & \Sigma_2\end{bmatrix} = \begin{bmatrix}\Sigma_s & 0\\ 0 & \Sigma_f\end{bmatrix} + \begin{bmatrix}O(\varepsilon) & O(\varepsilon^{1/2})\\ O(\varepsilon^{1/2}) & O(\varepsilon)\end{bmatrix} \tag{3.37}$$

Thus, for sufficiently small $\varepsilon, \hat{T}^{-1}\bar{P}\hat{T}^{-T} \approx \hat{T}^{T}\bar{Q}\hat{T} \approx diag(\Sigma_0, \Sigma_2) = diag(\Sigma_s, \Sigma_f) + O(\varepsilon)$.

3.2 Improved Method for Balancing Singularly Perturbed Linear Systems

The approximate balancing transformation technique for linear singularly perturbed systems of [3] was based on the approximate slow and fast controllability and observability gramians both obtained by solving the algebraic Lyapunov equation, defined in (3.38) and (3.39) respectively that is

$$\begin{aligned} A_0\bar{P}_{11} + \bar{P}_{11}A_0^T + B_0B_0^T &= 0\\ A_{22}\bar{P}_{22} + \bar{P}_{22}A_{22}^T + B_{22}B_{22}^T &= 0 \end{aligned} \tag{3.38}$$

$$\begin{aligned} A_0^T\bar{Q}_{11} + Q_{11}A_0 + C_0^TC_0 &= 0\\ A_{22}^T\bar{Q}_{22} + Q_{22}A_{22} + C_{22}^TC_{22} &= 0 \end{aligned} \tag{3.39}$$

Applying the Chang transformation to the exact controllability (3.17) – (3.19) and observability gramians , we can obtain the exact slow and exact fast reduced order Lyapunov equations as presented in Section 1.6.1. For the controllability gramians we have

$$\begin{aligned} 0 &= a_sK_{c\_s} + K_{c\_s}a_s^T + b_sb_s^T\\ 0 &= \varepsilon a_sK_{c\_2} + K_{c\_2}a_f^T + b_sb_f^T\\ 0 &= a_fK_{c\_f} + K_{c\_f}a_f^T + b_fb_f^T \end{aligned} \tag{3.40}$$

And for the observability gramians we obtain

$$\begin{aligned} 0 &= a_s^T K_{o\_s} + K_{o\_s} a_s + c_s^T c_s \\ 0 &= \varepsilon a_s^T K_{o\_2} + K_{o\_2} a_f + c_s^T c \\ 0 &= a_f^T K_{o\_f} + K_{o\_f} a + c_f^T c \end{aligned} \tag{3.41}$$

where

$$\begin{bmatrix} a & 0 \\ 0 & \frac{1}{\varepsilon} a_f \end{bmatrix} = TAT^{-1}, T^{-T} Q T^{-1} = \begin{bmatrix} q_1 & q_2 \\ q_2^T & q_3 \end{bmatrix}, T^{-T} P T^{-1} = \begin{bmatrix} K_1 & \varepsilon K_2 \\ \varepsilon K_2^T & \varepsilon K_3 \end{bmatrix} \tag{3.42}$$

T comes from the Chang transformation defined in Section 1.6

$$T = \begin{bmatrix} I - \varepsilon HL & -\varepsilon H \\ L & I \end{bmatrix} \tag{3.43}$$

L and H satisfy the following algebraic equations

$$\begin{aligned} A_{22} L - A_{21} - \varepsilon L (A_{11} - A_{12} L) &= 0 \\ H A_{22} - A_{12} + \varepsilon (HLA_{12} - A_{11} H + A_{12} LH) &= 0 \end{aligned} \tag{3.44}$$

References providing solutions to the above equations are presented in Section 1.6. Using the results (3.40) – (3.44) we can find the exact gramians of the system

$$P_{exact} = T^T K_c T, \qquad Q_{exact} = T^T K_o T \tag{3.45}$$

then

$$\sigma_i^2 = \lambda_i (P_{exact} Q_{exact}) \tag{3.46}$$

The square root of (3.46) will give us the exact Hankel singular values of the system. Using the exact controllability and observability gramians obtained in terms of pure slow and pure fast gramians we will be able to obtain the exact balancing transformation, and hence improve the approximate balancing of the singularly perturbed system of Shahruz and Behtash [3].

3.3 Balancing Transformation via the Chang Transformation Approach

The Chang transformation method was outlined in Section 1.6. It can be used to completely decouple a singularly perturbed system such as the one in (1.39). The Chang transformation method included $O(\varepsilon)$ whereas the technique presented by Shahruz and Behtash omits it hence we would expect more accurate results. In other words we will see the following relations between the approximate matrices and the ones obtained through the exact system decomposition into slow and fast subsystems

$$\begin{aligned} A_s &= A_0 + O(\varepsilon) & A_f &= A_{22} + O(\varepsilon) \\ B_s &= B_0 + O(\varepsilon) & B_f &= B_{22} + O(\varepsilon) \\ C_s &= C_0 + O(\varepsilon) & C_f &= C_{22} + O(\varepsilon) \end{aligned} \tag{3.47}$$

The matrices from (3.47) are defined in (3.48)

$$\begin{aligned} A_s &= A_1 - A_2 L, & A_f &= A_4 + \varepsilon L A_2 \\ B_s &= B_1 - H B_2 - \varepsilon H L B_1, & B_f &= B_2 + \varepsilon L B_2 \\ C_s &= C_1 - C_2 L, & C_f &= C_2 - \varepsilon C_2 L H + \varepsilon C_1 H \end{aligned} \tag{3.48}$$

With this information we can investigate the gramians of the slow and fast subsystems by solving the decoupled Lyapunov differential equations and improve the accuracy of [3].

Chapter 4

4. Conclusions

Fuel cell systems' mathematical models are usually of large order and that makes them impractical for efficient study. In this thesis we presented a theoretical approach on how to reduce the order of an 18^{th}- order fuel cell – fuel processing system developed by the University of Michigan without compromising the original behavior of the system.

First we investigated order-reduction using the balancing transformation and balancing residualization techniques. We compared the step and impulse responses of the reduced-order systems and the full-order system and concluded that the reduced system retained the original system's dynamics to high accuracy. The suboptimal gain was also observed and the results showed that it remained unchanged even when the system was reduced down to 6^{th} order.

In the second part of the study we demonstrated how to put the linear system in singularly perturbed form. We investigated the approximate gramians and balancing transformation developed in [3] and then provided a method to evaluate the exact gramians and balancing transformation by utilizing the Chang transformation.

Bibliography

[1] B. D. O. Anderson and Y. Liu, "Singular perturbation approximation of balanced systems," in *Proceedings of the 28th Conference on Decision and Control*, 1989.

[2] P. V. Kokotovic, R. E. O'Malley and P. Sannuti, "Singular perturbations and order reduction in control theory - an overview," *Automatica,* vol. 12, pp. 123-132, 1976.

[3] S. M. Shahruz and S. Behtash, "Balanced realizations of singularly perturbed systems," *International Journal of Control,* vol. 49, no. 1, pp. 207-217, 1989.

[4] Z. Gajic and M. Lelic, "Improvement of systems order reduction via balancing using the method of singular perturbations," *Automatica,* vol. 37, pp. 1859-1865, 2001.

[5] Z. Gajic and T. Grodt, "The recursive reduced-order numerical solution of the singularly perturbed matrix differential Riccati equation," *IEEE Transactions on Automatic Control,* vol. 33, no. 8, pp. 751-754, 1988.

[6] H. Khalil, Nonlinear Systems, New Jersey: Prentice-Hall, 2002.

[7] A. Sinha, Linear Systems: Optimal and Robust Control, Florida: CRC Press, 2007.

[8] F. Szidarovszky and A. T. Bahill, Linear Systems Theory, Florida: CRC Press, 1992.

[9] Z. Gajic and M. Qureshi, Lyapunov Matrix Equation in Stability and Control, California: Academic Press, 1995.

[10] Z. Gajic and T. Nguyen, "Solving the singularly perturbed matrix differential riccati equation: A Lyapunov equation approach," in *IEEE Transactions on Automatic Control*, 2010.

[11] J. M. A. Scherpen, "Balancing for nonlinear systems," *Systems & Control Letters,* vol. 21, pp. 143-153, 1993.

[12] V. Kecman, S. Bingulac and Z. Gajic, "Eigenvector approach for optimal control of singularly perturbed and weakly coupled linear systems," in *Automatica*, 1999.

[13] Z. Gajic, "Numerical fixed point solution of linear quadratic gaussian control problem for singularly perturbed systems," in *International Journal of Control,* 1986.

[14] G. Strang, Linear Algebra and Its Applications, Salt Lake City: Brooks Cole, 2005.

[15] J. T. Pukrushpan, A. G. Stefanopoulou and H. Peng, "Modeling and Control for PEM Fuel Cell Stack System," in *Proceedings of the American Control Conference*, Anchorage, 2002.

[16] N. S. Nise, Control Systems Engineering, Hoboken: Wiley, 2010.

[17] A. Tewari, Modern Control Design with Matlab and Simulink, Hoboken: Wiley, 2002.

[18] M. El-Sharkh, A. Rahman, M. Alam, P. Byrne, A. Sakla and T. Thomas, "A dynamic model for a stand-alone PEM fuel cell power plant for residential applications," *Journal of Power Sources*, no. 138, pp. 199-204, 2004.

[19] Z. Gajic, *Lecture Notes on Fuel Cells*, New Brunswick, 2010.

[20] B. D. O. Anderson and Y. Liu, "Controller reduction: concepts and approaches," *IEEE Transactions on Automatic Control*, vol. 34, no. 8, pp. 802-812, 1989.

[21] J. K. Astrom and R. M. Murray, Feedback Systems: An Introduction for Scientists and Engineers, Princeton: Princeton University Press, 2008.

[22] Y. Li, L. Wang and G. Yang, "Sub-optimal linear quadratic control for singularly perturbed systems," in *Proceedings of the 40th IEEE Conference on Decision and Control*, Orlando, 2001.

[23] G. Tang and Z. Lou, "Suboptimal control of linear systems with state time-delay," in *IEEE International Conference on Systems, Man, and Cybernetics*, Tokyo, 1999.

[24] H. Trinh and M. Aldeen, "A balancing realization approach to decentralized control of interconnected systems," in *International Conference on Intelligent Control and Instrumentation*, Singapore, 1992.

[25] A. Saberi and K. Hassan, "Quadratic-type lyapunov functions for singularly perturbed systems," *IEEE Transactions on Automatic Control*, vol. 29, no. 6, pp. 542-548, 1984.

[26] S. Gugercin and A. Antoulas, "A survey of balancing methods for model reduction," in *Proceedings of European Control Conference*, Cambridge, 2003.

[27] J. Phillips, L. Daniel and M. L. Silveira, "Guaranteed passive balancing

transformations for model order reduction," *IEEE Transactions on Computer-Aided Design of Integrated Circuits and Systems,* vol. 22, no. 8, pp. 1027-1041, 2003.

[28] J. B. Siegel, A. G. Stefanopolou and S. Yesilyurt, "Modeling and experiments of voltage transients of pem fuel cells with the dead-ended anode," in *Proceedings of the 9th Fuel Cell Science, Engineering and Technology Conference*, Washington D.C., 2011.

[29] B. A. McCain, A. G. Stefanopoulou and I. V. Kolmanovsky, "On the dynamics and control of through-plane water distributions in pem fuel cells," *Chemical Engineering Science,* vol. 63, no. 17, pp. 4418-4432, 2008.

[30] V. Tsourapas, A. G. Stefanopoulous and J. Sun, "Model-based control of an integrated fuel cell and fuel processor with exhaust heat recirculation," *IEEE Transactions on Control Systems Technology,* vol. 15, no. 2, pp. 233-245, 2007.

[31] J. T. Pukrushpan, A. G. Stefanopoulou and S. Varigonda, "Control-oriented model of fuel processor for hydrogen generation in fuel cell applications," in *IFAC Symposium in Adavnces in Automotive Systems*, Salerno, 2004.

[32] J. T. Pukrushpan, A. G. Stefanopoulou and H. Peng, "Control of fuel cell breathing," *IEEE Control Systems Magazine,* pp. 30-46, April 2004.

[33] J. T. Pukrushpan, A. G. Stefanopoulou and H. Peng, Control of Fuel Cell Power Systems: Principles, Modeling, Analysis and Feedback Design, Springer: New York, 2010.

[34] J. T. Pukrushpan, A. G. Stefanopoulou and H. Peng, "Simulation and analysis of transient fuel cell system performance based on a dynamic reactant flow model," in *Proceedings of the 2002 IMECE Conference*, Louisiana, 2002.

[35] B. Moore, "Principal component analysis in linear systems: controllability, observability, and model reduction," *IEEE Transactions on Automatic Control,* vol. 26, no. 1, pp. 17-32, 1981.

[36] A. J. Laub, M. T. Heath, P. C. C. and R. C. Ward, "Computation of system balancing transformations and other applications of simultaneous diagonalization algorithms," *IEEE Transactions on Automatic Control,* vol. 32, no. 2, pp. 115-122, 1987.

[37] W. K. Na and B. Gou, "Feedback-linearization-based nonlinear control of PEM fuel cells," *IEEE Transactions on Energy Conversion,* vol. 23, no. 1, pp. 179-190, 2008.

[38] L. Chiu and B. M. Diong, "An improved small-signal model of the dynamic behavior of PEM fuel cells," in *Industry Applications Conference*, Salt Lake City, 2003.

[39] P. Kokotovic, H. Khalil and J. O'Reilly, Singular Perturbation Methods in Control: Analysis and Design, Philadephia: Society for Industrial and Applied Mathematics, 1987.

[40] Z. Gajic, A. Muhammad, Z. Al Jarrah and S. Alaraj, "System-order reduction via balancing and suboptimal control of a 75 kW PEM fuel cell," in *The 2011 International Conference on Water, Energy and the Environment*, Dubai, 2011.